Electrospinning of Composite Materials

Christiansen, Lasse

DOI (link to publication from Publisher):
10.54337/aau429194343

Publication date:
2021

Document Version
Publisher's PDF, also known as Version of record

ELECTROSPINNING OF COMPOSITE MATERIALS

BY
LASSE CHRISTIANSEN

DISSERTATION SUBMITTED 2021

AALBORG UNIVERSITY
DENMARK

ELECTROSPINNING OF COMPOSITE MATERIALS

by

Lasse Christiansen

AALBORG UNIVERSITY
DENMARK

Dissertation submitted

Dissertation submitted: February 2021

PhD supervisor: Associate Prof. Peter Fojan,
Aalborg University

PhD committee: Associate Professor Thomas Soendergaard (chairman)
Aalborg University

Professor Ioan-Stefan Voicu
University Politehnica of Bucharest

Professor Ioannis S. Chronakis
Technical University of Denmark

PhD Series: Faculty of Engineering and Science, Aalborg University

Department: Department of the Build Environment

ISSN (online): 2446-1636
ISBN (online): 978-87-7210-908-4

Published by:
Aalborg University Press
Kroghstræde 3
DK – 9220 Aalborg Ø
Phone: +45 99407140
aauf@forlag.aau.dk
forlag.aau.dk

Printed in Denmark by Rosendahls, 2021

ENGLISH SUMMARY

This thesis reports on electrospinning of composite materials, in the context of the increasing focus on energy-efficient buildings, outlined e.g. in the Danish building regulations (Byg2020) and the United Nations world goals 11 (Sustainable cities and communities) and 13 (Climate action). These programs all require housing to consume less energy for heating in the future. The building footprint area, however, is generally not allowed to increase. Using the traditional insulation materials, the insulated walls are thickened, leading to a loss of net area inside the house.

When focusing on preserving the size of living area in general the development of more efficient insulation materials is vital. These efficient materials require low thermal conductivity, and here vacuum insulation panels dominate the market today. Shortcomings have been experienced with vacuum insulation panels though: they are difficult to retrofit and come with a risk of leakage causing a concomitant risk of reduced insulation properties. Hence, other materials are needed to ensure a versatile portfolio of available insulation materials. Aerogel materials could fill this gap, but their brittleness, low mechanical strength and wetting behaviour makes them difficult to use.

The aim of this project has been to develop methods to enhance the mechanical properties of aerogel by embedding aerogel particles in a polymer fibre matrix. Different electrospinning variants as a production method for composite insulation materials have been developed. The different electrospinning variants have been tested with different types of aerogel, and the produced fibre materials have been characterised. Various characterisation techniques are used to determine the thermal and mechanical properties of the fibres. The electrospinning variants have also been upscaled by going from single needle prototypes to multi-needle electrospinning in the case of both melt and solvent electrospinning.

The results of these experiments are documented in four scientific papers, of which three have been published in scientific journals. Three papers address the production of electrospun fibres, containing aerogel, through melt and solvent electrospinning, while the last paper addresses the link between gas permeability and thermal conductivity in fibre materials.

In conclusion, the results presented in this thesis contribute to the scientific knowledge of composite material electrospinning, and the understanding of the thermal properties of porous fibre materials. The development of the new production methods can aid future research in and production of electrospun materials.

DANSK RESUME

Denne afhandling er skrevet med det formål at fortælle om elektrospinning af kompositmaterialer i sammenhæng med bygningsisolering og energieffektivitet. Dette ses eksempelvis i Det Danske Bygningsreglement, Byg2020, FN's verdensmål 11 (bæredygtige byer og samfund) og 13 (klima). Der er et krav om mindre udledning af kuldioxid, som følge af opvarmning og nedkøling af bygninger, men samtidig må bygningens sokkelareal ikke øges. Hvis man vil isolere yderligere med traditionelle isoleringsmaterialer, vil sokkelarealet blive tykkere, hvilket vil medføre en uønsket nedgang i beboeligt areal.

Hvis man har fokus på netop at opretholde det beboelige areal, er det derfor vigtigt med mere effektive isoleringsmaterialer. Denne type materialer skal først og fremmes have en lav varmeledningsevne, og her er det bedste bud i dag vakuumisoleringspaneler. Vakuumisoleringspaneler har dog også kendte ulemper; eksempelvis er de svære at tilpasse, og de har en indlejret risiko for lækage. Derfor har byggeriet brug for alternative materialer, som kan bruges hvor dette udgør et problem. Et bud på et sådant materiale, kunne være aerogel, men materialet er for sprødt, har lav mekanisk styrke og suger let fugt, hvilket gør det vanskeligt at anvende i byggebranchen.

Formålet ned dette projekt har været at udvikle en metode, til at forbedre aerogelens mekaniske egenskaber. Dette sker ved at indlejre aerogel partikler i en elektrospundet fibermåtte. For at opfylde dette formål, er der udviklet elektrospinningsvariationer, som er blevet testet med forskellige typer aerogel. De resulterende fibre er blevet karakteriseret ved forskellige metoder, og elektrospinningsvarianterne er efterprøvet i flernålsopstillinger for både smelte- og opløsningselektrospinning.

Resultatet af disse eksperimenter er udgivet i fire artikler. Tre artikler er publiceret, og én er indsendt til bedømmelse. Af de fire handler de tre om elektrospinningsvariationer med både opløsning og smelte, mens det sidste fortæller om sammenhængen mellem luftpermeabilitet og varmeledningsevne for fibermaterialer.

Resultaterne af dette arbejde bidrager til den samlede viden om kompositelektrospinning, og forståelsen af varmeledning i porøse fibermaterialer. Udviklingen af nye elektrospinningsvarianter kan støtte den videre udvikling af nye materialer.

.ACKNOWLEDGEMENTS

This is the final account of my journey through a Ph.D.-fellowship. Some people deserve acknowledgement, as I have not undertaken this journey alone.

Firstly, I would like to thank Peter Fojan and Mette Herold-Jensen for giving me the chance to become a part of this project. I would also like to thank the organisations of Gabriel A/S and HiCON A/S, and Anna Fricke and Tommy Bæk Hansen, for their collaboration both during the application period, and later in during the Ph.D. period.

Furthermore, I would also like to thank the staff at Civil Engineering at Aalborg University and Soil Physics at Aarhus University for their collaboration. I appreciate the contributions they have made, and their qualified and constructive suggestions have helped me find a direction for the work proposed.

I would also like to thank my colleges and the organisation at UCN for supporting me in the process of completing this work after my position at Aalborg University ended. Without their support, this thesis would have lived a quiet life in a cabinet drawer, only half finished.

As a last note, I would like to thank my family for their patience, support, and care throughout the process, while my focus has been elsewhere.

This project has been financially supported by The Danish Board of Innovation, with funding number J.no. 0052-2012-3.

TABLE OF CONTENTS

FOREWORD

The project, entitled *Electrospinning Novel Composite Materials*, aims to investigate the possibilities for creating composite materials by combining polymers with silica-based aerogels through electrospinning. This PhD-thesis has been part of the project, sponsered by the Danish Innovation Fund, and is a collaboration between Aalborg University, Gabriel A/S and HiCON A/S. The main focus of the project has been towards research relevant for the production of insulation material based on the combination of aerogel particles and polymers, where the industrial partners have been focused on the incorporation of these materials into their product portfolio.

In general terms, this project has aimed to answer the question: **Where are the limits of aerogel-polymer based composite fibres, and the electrospinning methodology for scalable production?**

This question has been answered in four scientific papers. Three are published at the time of the handing in of this thesis. Furthermore, this thesis includes a state- of-the-art review of the electrospinning process, the insulation materials and a chapter covering relevant theory. This chapter of theory covers the electrohydrodynamic process of electrospinning, gas and thermal transport and mechanical properties of composite fibre materials.

CHAPTER 1. – ELECTROSPINNING STATE-OF-THE-ART AND THEORY

In its most basic form, electrospinning needs a curved liquid surface in an electric field (1). As liquid is polarised or charged, a Taylor Cone can emerge (2), and fibres start propagating away from the curved surface. The state of the art within the field of electrospinning has shown a fast development within recent years, as the well-known technique has both been upscaled for industrial applications and developed further intensely to produce new fibre types and composite materials.

In summary, electrospinning can be used to produce varying fibres for different applications, ranging from medical, pharmaceutical, filtration, and construction applications. This also includes aerogel/polymer composite fibres. The various electrospinning setups have experienced a considerable evolution during the last decade, where high-throughput devices and advanced geometries of fibres have been implemented in various processes. But still, the potential for future developments of novel fibre types and production methods.

1.1. TAYLOR CONE FORMATION

Before the electrospinning starts, a curved liquid surface exists in an electric field. The Taylor cone forms when the electrostatic pressure, p_{es}, between a charged liquid and a charged electrode surpasses the surface tension pressure or Laplace pressure, p_{γ}. Then a thin fibre emerges, and this is the start of the electrospinning. The electrostatic pressure is given by

$$p_{es} = \frac{\epsilon_0}{2} \cdot E^2, \qquad 1.1.1$$

where E is the electrostatic field, and $\epsilon_0$is the vacuum permeability. The surface tension pressure is given by

$$p_{\gamma} = \gamma \cdot \kappa, \qquad 1.1.2$$

where γ is the surface tension, and κ is the curvature of the droplet (3). In the case of electrostatics, Taylor did experimental work showing that this equilibrium happens at droplet angle of 49.3°(2) compared to the surface, and this is mathematically proven in the case of electrostatics by Wilm and Mann (3).

1.1.1. ELECTRIC FIELD

Electrospinning occurs in a static electric field. This electrostatic field depends on two variables: the distance between the liquid and the collector, and the applied potential. The electrostatic field is defined as

$$E(\boldsymbol{r}) = -\nabla\varphi(\boldsymbol{r}), \qquad 1.1.3$$

where $\varphi(\boldsymbol{r})$ is the electrostatic potential. As the potential is an experimental parameter defined by the researcher, the 1D electrostatic field can be calculated as

$$E(r) = -\frac{\varphi}{r}. \qquad 1.1.4$$

By applying this equation, electrospinning can be achieved both by increasing the potential and by decreasing the distance. As the droplet is charged in the field, a force acts on a given volume element with the magnitude of

$$F(r) = qE(r) = -q\frac{\varphi}{r}, \qquad 1.1.5$$

where q is the charge of the volume element.

The same electrostatic field that makes the fibre emerge from the droplet acts on the charged jet. As the jet is composed of liquid material, it experiences a viscous stretch (4).

1.1.2. VISCOSITY OF LIQUID PHASES

This viscous resistance in an element *a*, in a liquid, works in the opposite direction of the electrostatic force as

$$dF_i = \sigma'_{ij}\, n_j \,\mathrm{d}a, \qquad 1.1.6$$

where dF_i is the viscous force, σ'_{ij} is the stress tensor and n_j is the normal vector of the surface element. The stress tensor is defined as

$$\sigma'_{ij} = \eta\left(\partial_j v_i + \partial_j v_i - 2/3\delta_{ij}\partial_k v_k\right) + \zeta\,\partial_k v_k, \qquad 1.1.7$$

where η is the dynamic viscosity (friction due to shear stress), ζ is the secondary viscosity (friction due to compression) and *v* is the velocity field in the *i*, *j* and *k* directions.

This means that the resistance to the movement of an element of fluid, in comparison to a neighbouring element, is proportional to the viscosity if no change in density is present (incompressible fluids).

The viscosity is dependent on the temperature of the fluid, as well as the properties of the fluid component. The length of polymer chains and solvent concentrations are dominant factors for these properties, and hence, the stretch of the fibre depends thereon. Literature states that decreasing viscosity leads to decreasing fibre diameters, which corresponds to the equations above, stating that the resistance to stretch is increased upon a viscosity increase (5). The same factors influencing the viscosity are also tightly coupled to the surface tension of a solution.

1.1.3. SURFACE TENSION

The surface tension of a solution is defined as the Gibbs free energy (G) derived per unit of surface area (A) at a fixed pressure and temperature (5):

$$\gamma = \frac{\partial G}{\partial A_{T,p}}. \qquad 1.1.8$$

Hence, the Gibbs free energy is defined as

$$G(p,T) = U + pV - TS, \qquad 1.1.9$$

where U is the internal energy, p is the pressure, V is the volume, T is the temperature and S is the entropy of the system, which is defined as

$$S = k_B ln(\Omega), \qquad 1.1.10$$

where k_B is the Boltzmann constant and Ω is the number of available configurations of the system (6).

By combining equations 1.1.9 and 1.1.10, it can be seen from equation 1.1.8 that the surface tension decreases with temperature, and increased pressure increases the surface tension.

1.1.4. CURVATURE

The curvature of a droplet is inversely proportional to its radius and is defined as

$$\kappa = \frac{1}{r_{droplet}}. \qquad 1.1.11$$

The larger the radius, the lower the curvature, and, by extension, the lower the electrostatic pressure. If the droplet is assumed to be an ellipsoid, the smallest radius will

be in the centre, and if the electrostatic pressure surpasses the pressure of the surface tension a Taylor Cone will emerge from this point (3).

1.2. ELECTROSPINNING MATERIALS

The first report on electrospinning of a polymer or glass melt is dating back to 1887 (1), and was patented in the early 19th hundreds (7). The increased interest in polymer based materials (8), glasses (9), food materials (10), and ceramics (11) has fuelled the further development and industrial implementation of the electrospinning process during the last decades.

1.2.1. POLYMER MATERIALS

Polymer fibres are spun from both melt and solution of most polymer materials. It is reported that both linear (12) and crosslinked (13) polymers have been spun under various conditions, producing fibres for a wealth of applications. An overview of this can be seen in Table 1.

Table 1 - Electrospun polymer materials and examples of applications.

Polymer name	Abbreviation	Solution	Melt	Application	Reference
acrylonitrile butadiene styrene	ABS	X		Filtration	(14,15)
polyamide	PA	X	X	Filtration, textile, thermoregulation	(16–21)
polyacrylonitrile	PAN	X		Battery electrode, catalyst	(22–24)
poly(methyl methacrylate)	PMMA	X	X	Enzyme immobilisation	(12,25–28)
cellulose acetate	CA	X	X	Biomolecule immobilization, tissue engineering, bio-sensing, nutraceutical delivery, bio separation	(29–32)
cellulose acetate butyrate	CAB	X		Bio scaffolding	(33)
polyethylene	PE	X	X	Thermoregulation	(18,28,34)
polyethylene oxide	PEO	X		Antibacterial textiles	(35,36)

polycarbonate	PC	X		Filtration	(37–40)
polytetrafluoro-ethylene	PTFE	X		Oil-water separation, nanogenera-tors	(19,37,41–44)
ethylene vinyl ac-etate	EVA	X		Filtration	(16,45)
poly(vinyl alco-hol)	PVA	X		Battery membrane	(46–48)
polybutylene ter-ephthalate	PBT	X		Extraction	(49–51)
polycaprolactone	PCL	X	X	Biomedical	(52–54)
poly(ether ether ketone)	PEEK		X	Avoid sulfonation	(55)
poly(aryl ether sulfone)		X		Proton exchange membrane	(56)
polyetherimide	PEI	X		Filtration, batteries	(48,57)
polyethylene ter-ephthalate	PET	X	X	Filtration	(58,59)
polyimide	PI	X	X	Battery membrane	(28,60,61)
polylactic acid	PLA	X		Filtration	(45,62,63)
polyoxymethylene	POM	X			(64)
polypropylene	PP	X	X	Surgery, biomedical, textile	(28,65–68)
polystyrene	PS	X		Distillation, oil-water separation	(69,70)
polyvinylchloride	PVC	X		Batteries	(71,72)
starch		X		Textile, filtration	(73)
silk		X		Bioscaffold	(74)
gelatine		X		Membranes	(75)

Thermosets can also be part of the electrospinning process (76). Polymer fibres can be spun directly from resin, where the curing is inhibited before or during the collection process (77,78). The process can also include the co-spinning of a thermoset and a thermoplast (79,80).

1.2.2. FABRICATION OF OTHER FIBRE MATERIALS

Several other types of fibre materials can be achieved from the electrospinning process. The direct electrospinning of glass fibres is referenced by Boys (1), and the production of fibres in the nanometre range have been reported for silicon oxide (9,81) boron trioxide (28,82) and As_3S_7 chalcogenide (83).

Other types of materials have been fabricated by different types of post-processing of fibres spun from solutions containing, e.g., metal ions. This post-processing has enabled creation of ceramic nanofibers from ZnO (11,84), SnO_2-ZnO (85), CdS-TiO_2 (86), yttria-stabilized zirconia (87,88), NiO (87) and SiC (89).

1.3. CURVATURE FORMATION AND FEEDING

The electrospinning process occurs when the Coulomb force surpasses the surface tension, and a Taylor Cone emerges from the liquid (2). For this to happen, the liquid surface should have a curvature, which can either be a droplet (e.g.) at the end of a needle or various needleless setups (28).

1.3.1. NEEDLE ELECTROSPINNING

A simple way to perform electrospinning is by placing a droplet of liquid material at the end of a needle. This droplet can deplete through the spinning process, and hence, a liquid feed can be applied through a syringe pump for a solution or an extruder in the case of melt electrospinning (28).

This simple single-needle setup can be easily modified and upscaled. An additional needle can be mounted inside the outer needle (90,91). Such a coaxial setup can produce several fibre types with one material on the outside and another one on the inside (49,90,92). The coaxial setups exist in further variations, where additional inner needles are added, creating either multilayer fibres, e.g. triaxial fibres (90,92,93). In addition to this, parallel inner needles can be inserted to create an island-in-the-sea fibre, where similar or different core materials form island-like cavities in a polymer sea are created (94,95). These different configurations are depicted in Figure 1-1.

Several needles can also be added to the process with either the same or different polymer materials (96,97). The addition of extra needles to the setup provides a higher material throughput and enables the creation of a material consisting not only of a single fibre material.

The needle(-s) and/or collector can furthermore be moved to create a pattern of the electrospun fibres (98,99). Especially for near field electrospinning, this can create patterns and fibre stacks, e.g. for plasmon contraption (100) or scaffolding (101).

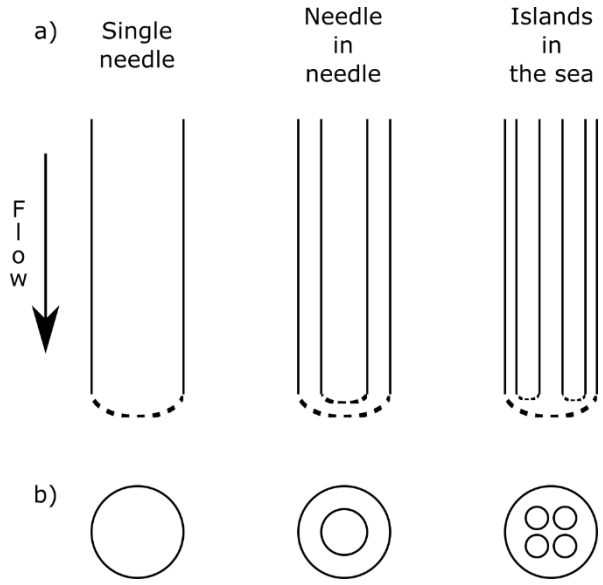

Figure 1-1 - An overview of needle setups for electrospinning: a) side view and b) bottom view.

1.3.2. NEEDLELESS ELECTROSPINNING

There are also techniques to create a curved surface without creating a droplet at the end of a needle. These techniques create a curvature of the liquid, and then the electrospinning can take place as usual. Typically, these techniques are used to produce one-phase fibres without cores or side-by-side parts, but on the other hand, it is created to yield a high throughput (68,102).

One method to create a spiked surface is to deposit a thin layer of polymer solution on top of a ferrofluid, and then place this on top of a permanent magnet. As the ferrofluid creates a pattern of spikes aligned in the magnetic field, several curvatures coved in the polymer is created, and fibres can be drawn from these (103).

This limitation can be overcome in various ways, e.g. by rotating a drum, disk or gear in a polymer melt or solution (68,102,104). The addition of air bobbles into the electrospinning liquid can also create this effect (105). If there is a potential difference between the curved liquid surface and the collector, fibres can emerge and create higher throughput than achievable by traditional needle electrospinning

Commercial apparatus for this process can be obtained from several vendors, and, e.g. the Elmarco Nanospider technique (106), have been patented (107) and can be obtained from a commercial supplier.

1.3.3. CENTRIFUGAL ELECTROSPINNING

Another method to create electrospun fibres is to use a rotating spinning nozzle, and a charged collector barrel. By rotating the nozzle at a high angular velocity, and applying an electrical potential, fibres can be created with the geometrical features of side-by-side or coaxial needle electrospinning, while having a production rate in the range of needleless electrospinning (108,109).

The method applies high angular velocities, between 3000 and 12000 RPM, and can yield throughputs up to 1000 times higher than conventional needle electrospinning for fibre diameters down to 80 nm (108,109).

1.4. LIQUIDFICATION TECHNIQUES

For a fibre to emerge a liquid material must be present, and at the same time it must solidify into a fibre before it hits the collector. This liquification can happen in several ways, including solution, melt, sol-gel and supercritical electrospinning.

1.4.1. SOLUTION ELECTROSPINNING

A simple method to produce electrospun fibres is from a solution. This solution can be based on different solvents, e.g. water (36), chloroform (110), acetone (110) or diethyl ether (110), as well as mixtures between different solvents (110).

Solution electrospinning can be done from most thermoplastic materials, and dependent on the solvent, different components can be added to the solution; nanoparticles, salts and ions, antibiotics, proteins and stem cells (110,111).

Both needle and needleless electrospinning are compatible with solution electrospinning, where the solution can be pumped into the needle or a container from where the needleless apparatus is fed (96,102,108). Commercial equipment can be obtained

from several vendors for both research purposes and mass production, and products based on solution electrospinning have hit the market (108,112).

Most types of fibres can be spun though solution electrospinning, including the side-by-side and coaxial fibre types (92,113). The compatibility between the solvents must be taken into account, as non-mixing fluids are beneficial for the creation of core-shell fibres, while more mixable fluids creates a more interconnected fibre by (e.g.) side by side spinning (91).

In general, solution electrospinning can produce nano-fibres with diameters down to 50 nm in far-field electrospinning (28). It is also applicable for nearfield electrospinning, where the choice of solvent enables fibres to stack together and form nano- or micro-structures (99).

For industrial purposes, the solvent needs to be recaptured. This is an obstacle for the implementation of solvent electrospinning in more extensive industrial settings, as the focus of the textile industry on the field have shown during recent years (28,109).

1.4.2. MELT ELECTROSPINNING

Melt electrospinning can be performed from thermoplastic polymers as well as glass melts. The material should be heated to above melting temperature and drawn into a fibre by the applied potential, as with solution electrospinning. As the emerging fibre cools down, the viscosity of the raw material drops and the fibre stretches less and less as it emerges. This process generally creates fibres with diameters down to 500 nm (28).

Different materials can be added to the polymer blend to create a composite in the melt electrospinning process. These additives can be strontium-substituted bioactive glass into melt-electrospun polycaprolactone fibres (114) and titanium dioxide in a polypropylene fabric (115).

The melting of the polymer can take place in different ways (28). The polymer can be supplied by air pressure, through a heated syringe pump, through a screw extruder or by a mechanical filament feed. It can be heated by either electric heating elements, circulating fluids or a focused laser beam, and, as the case with solution electrospinning, the spinneret can move (28,116).

Melt electrospinning is well suited for both needle and needleless electrospinning and has been of particular interest recently as the process does not involve solvents

(28,99). As solvent recapture isn't necessary in this process, it can be applied with fewer environmental concerns (28).

Melt electrospinning can be used to produce one-phase fibres, as well as core-shell fibres with both polymer and other core components. The side-by-side process can also be used (28,117).

1.4.3. OTHER METHODS

The liquification of the material for electrospinning is dominantly achieved by solvent and melt electrospinning, but other methods have also been described in the literature.

Supercritical CO_2 have been used to electrospin polydimethylsiloxane inside a pressure chamber (118). Supercritical CO_2 have also been used in combination with solvent electrospinning in order to electrospin (e.g.) hollow nanofibers in a single process (119).

Polymer fibres can also be electrospun by crosslinking resins during the process. This process can be used to spin (e.g.) polydimethylsiloxane or hybrid fibres (120,121), and can be combined with solvent electrospinning in a coaxial needle setup.

1.5. ELECTRIC FIELD

For the Coulomb force to surpass the surface tension and produce a Taylor cone from which a fibre can emerge, a significant potential difference must be applied within the electrospinning setup. A non-strict distinction between far- and near-field electrospinning can be applied, in order to treat two different domains of electrospinning. He et al. suggests a boundary at 50 mm (99), but the characteristics of the two processes change gradually.

1.5.1. NEAR-FIELD ELECTROSPINNING

Near field electrospinning is a variety of electrospinning defined by the shorter distance between the collector and the Taylor cone. This shorter distance removes the turbulent whipping of the fibre, and hence, the position on which the fibre is collected is determinable (99,100,122).

By using this method, a controlled deposition in patterns can be achieved by way of the electrospinning device and the collector. The process takes place at a lower voltage

than far-field electrospinning and has a lower production rate. The precise fibre deposition enables the production of small-scale components, e.g. biomedical scaffolds (123), optical waveguides (100) or electronic circuits (99,122).

1.5.2. FAR-FIELD ELECTROSPINNING

Far-field electrospinning is the electrospinning method, which is most often associated with the term electrospinning. The fibre propagates from the Taylor cone, and travels straight for a distance, after which it starts a more chaotic movement. This process requires a high voltage, it produces thin fibres down to 50 nm, and can be used for large-scale production. The process can be applied to most materials, with both solution, melt and sol-gel electrospinning (116).

1.5.3. ELECTRIC CONFIGURATIONS OF ELECTROSPINNING SETUPS

The potential difference required for electrospinning can be introduced in either the electrospinning nozzle, the collector or both. This can be done in six different configurations as see in Table 2.

Table 2 - Possible electrode configurations for electrospinning

Electrode configuration of spinneret	Electrode configuration of collector	Reference
+	G	(75,124)
+	-	(125)
G	+	(124)
G	-	(124)
-	+	(126)
-	G	(124)

Nonconducting collectors can also be introduced between the spinneret and an electrode with applied voltage or ground. This can be glass (127), silicon wafers (128), or even liquid solvents (1.6.4).

1.5.4. ADVANCED GEOMETRIES AND FIELD CONTROL

These simple electrospinning setups can be altered to gain further control over the electrospinning process, where both 3D field control and static field optimisations have been investigated (129).

One technique used to reduce the area in which the fibres were collected has been to introduce a ring of controllable electrodes, in order to reduce the loss of fibre material when using a fast rotating collector (129). This technique requires AC-voltage to be applied in order to overcome the repulsion between the fibres, which otherwise enables the collection of patterned, looping fibres through far-field electrospinning (129).

Another advanced technique is the Direct Write Near-field Electrospinning technique, where a moveable spinneret and a collector for melt electrospinning enables the formation of advanced fibre patterns. This technique draws on a whipping-free fibre path, where the fibre can be expected to land within a certain position with narrow tolerances. Due to this precision the technique is used for designable scaffolds. (54,130)

1.6. COLLECTION TECHNIQUES

The collection of the electrospun fibres can be performed in many different ways. The simplest form of collection is a plate. Various geometries of collectors have been introduced to produce patterned (131), aligned (132), or processed (133) fibres by electrospinning. (28,99)

These collection technics can be divided into subfields; stationary collectors and moving collectors. Furthermore, continuous collection systems have been created for industrial purposes, and non-solid collectors of liquids and gels have also been implemented. (28,99)

In general, most electrospinning collectors are composed of a metal, as they can serve as an electrode at the same time. Different materials can be placed in front of the electrode to collect the fibres. (28,99)

1.6.1. STATIONARY COLLECTORS

Stationary collectors are the simplest type of collectors. Seen from the tip of the Taylor cone, the collector can be a 2D plane (a plate, ring or similar) or a 1D setup (one or more line).

The 2D collector systems are used to create a nonwoven textile without any degree of ordering (14,29). The method is still widely used, as it enables the production of samples in a fast and efficient manner.

1D collector systems are consisting of sharp edges pointing towards the Taylor Cone. This can be in the shape of two parallel wires, plates or similar, and offer the advantage that fibres can be aligned between these elements (28,134).

1.6.2. MOVING COLLECTORS

Moving collection systems can be divided into two subcategories: collection systems, which move in cartesian coordinates (as in near-field electrospinning), and rotating collection systems.

The movement of the collector in X, Y and Z coordinates can be used to deposit ordered patterns of electrospun fibres (98). In near-field electrospinning with small deposition rates, this can be used to create highly aligned and even stacked fibre patterns, and hence enables the writing of (e.g.) electronic circuits (99). The control over the z coordinate also allows the potential to be controlled during electrospinning of thick fibre materials (135).

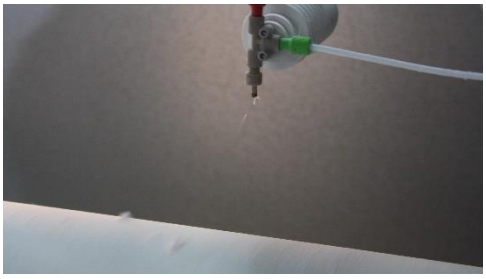

Figure 1-2 The rotating drum collector used in this project.

The use of rotating collectors for far-field electrospinning makes it possible to align the fibres spun by this turbulent process. If the collector is rotating with a speed comparable to the deposition rate of the fibres, the fibres can be aligned along the collection direction. This has been implemented for disk (33), drum (31,33) and aligned wires[OBJ][OBJ].Figure 2-2[OBJ] shows a rotating collector collector setup as has been used in this project.

1.6.3. CONTINUOUS COLLECTING SYSTEMS

For industrial purposes, the two types of collection methods described above must be altered in order to produce a continuous supply of electrospun fibres. The continuous collection is often vital for an industrial application, and hence, different techniques have been proposed.

Yarn from electrospun fibres can be spun in several ways. Funnel electrospinning is a method to produce nano-fibre yarn from the electrospinning process. A rotating funnel is used as the collector, and a hook goes into the centre of the funnel to pick up a thin thread. The hook takes the non-woven material and directs it towards a rotating thread collector on which it is fastened. As the funnel rotates perpendicular to the thread collector, the thread is twisted before it is deposited on the new collector (133). Another method is to spin it towards a suction apparatus, where the fibres are sucked into an airflow and transformed into yarn (68).

Another method for continuous collection is to spin onto a conveyer belt, which transport the electrospun fibres forward for postprocessing (137). This type of setup is commercially available (112), and finds various applications within the industry.

1.6.4. LIQUID COLLECTORS FOR WET SPINNING

Liquid collection systems can be used to collect fibres in need of further drying or curing. The liquid must not interact with the fibres, since that would dissolve the fibre rather than cure it (138,139). This technique can be used for both upscaled setups, where the spun fibres can float away from the spinning process and collected continuously, and in smaller experimental setups (138). For sol-gel fibres, in need of curing, the process of liquid collection enables them to cure before crosslinking with each other creating a mesh (120).

1.7. MICRO-STRUCTURES

On the micro-level many different fibre types exist. The simplest among these is the single-material fibre, but a large number of composite types with different geometrical features exist.

The introduction of a core material into a fibre has been presented, and methods to yield cores with up to five chambers are known (91). Initially, the method required a two-step process where a liquid was placed inside the polymer fibre and dried afterwards (93). Recent developments have shown that a gas jacket can be used to stabilise the electrospinning of polymer fibres with an air-core (90).

Side-by-side fibres have also been produced, and by altering the properties of one side these can become helical shaped (98). Fibres covered in a non-spinnable material like a thermoset shell can be produced (76), and added different components protein (10) or antimicrobial silver nanoparticles (32). This addition of microscopic components, smaller than the size of the fibre, have also been performed in combination with core-shell fibres, where the particles have been located both on the in- and outside of the

fibre (140). This can also be done with a ferrofluid, in order to create magnetic nanofibers (50,141).

In the case of particles with diameters higher than the diameter of the fibre, a few results have also been reported. The electrospinning of neckless-like structures with polystyrene beads embedded in a polymer fibre (142), and also stemcells (101), are examples of this.

1.7.1. AEROGEL COMPOSITE FIBRES

Aerogel is brittle and degrades into fine dust under mechanical load, and different attempts have been proposed to improve the mechanical properties of aerogels, including adding different elements to the gel at the molecular level (143–145), as well as by forming aerogel/fibre composites (146).

The addition of polymer fibres to aerogel materials has been performed in order to enhance mechanical properties of the brittle aerogel (147,148). This process has been improved to a level where the aerogel can be made elastic by applying electrospun fibres in a controlled 3D pattern (149), and the same goes for processes where existing textiles are coated with aerogel/polymer particles or fibres through electrospraying or -spinning (104).

Another way to produce electrospun aerogel composite fibres is to electrospin aerogel fibres containing a precursors, and finally obtain the aerogel fibres by supercritical drying (150). However, the direct incorporation into the core of electrospun fibres has not been previously reported.

Near-field electrospinning of highly aligned fibres have been proposed for use in areas like small- and large-scale energy collection, wearable devices, small scale electronics, design of microfluidics and light-emitting electrodes (99,100).

1.8. MECHANICAL PROPERTIES OF COMPOSITE MATERIALS

The mechanical properties of engineered materials, as insulation materials, is interesting on both the micro and the macro level. The overall material properties averages the micro-level mechanics between the matrix material and the inhomogeneities. These overall average properties are of interest when the material is applied as (e.g.) housing insulation (151,152).

On the microlevel, inhomogeneities defines an area with different physical properties than the surrounding matrix. If the matrix is bound to the inhomogeneity, there is continuous strain over the interface linking the inhomogeneity and the matrix, while

the stress can differ. As the inhomogeneities have other physical properties than the matrix material, and hence other criteria of failure, it can either absorb more or less of the load than the matrix (152).

While these effects take place at the particle level, where distances are small (and can be denoted as d), on a larger scale, D, the average properties are more interesting. If the features at the micro-level are much smaller than the sizes in which the material must be used, it can be considered as a homogeneous construction material. This is the case for wood, fibre reinforced polymer and many other materials (153).

However, the composite can be tested, or the overall properties estimated, from the composition to gauge these physical properties. These estimates of (e.g.) failure strength (a.k.a. Youngs Modulus) are notoriously hard to predict, but the Voigt and Reuss bonds provide a general region for estimation. The Voigt upper bond is given by

$$L_{effective} = \sum c_r L_r, \qquad 1.8.1$$

and the Reuss lower bond by

$$L_{effective} = \left[\sum c_r {L_r}^{-1}\right]^{-1}, \qquad 1.8.2$$

where $L_{effective}$ is the effective parameter, e.g. stiffness, c_r is the composition rate of the given component and L_r is the parameter of the same component (152,153).

The physical parameters of a mixture of two or more components can be expected to be between these two bounds, and hence, this can be used to predict the mechanical properties of (e.g.) new insulation materials.

CHAPTER 2. STATE-OF-THE-ART – THERMAL INSULATION

The state-of-the-art of insulation materials have recently moved from using a few, well-documented materials, towards a more diverse material library with special applications (154). Application of insulation materials in the building envelope is governed by a framework of laws covering insulation properties, flame resistance and moisture retention thresholds among others (155). These novel materials have to fulfil the aforementioned requirements, and nowadays are mainly based on vacuum insulation panels, low-conducting gas containing building elements or nano porous materials, as well as combinations thereof (154).

Due to the low thermal conductivity and high flame resistance, aerogel materials are of interest as insulation materials in buildings. Novel insulation materials have to decrease the thermal conductivity of the total building envelope, and hence allows for continued use of the same wall- and roof geometries (154).

2.1. CLASSIFICATION

Insulation materials must limit conduction, convection, and radiation of thermal energy to limit the overall heat transfer through (e.g.) a building envelope. The theory of thermal transport is expanded in **Fejl! Henvisningskilde ikke fundet.**. Different types of insulation materials limit different types of heat transfer. Insulation materials can be divided into reflection insulation and low conductivity/convection insulation (156,157).

2.1.1. REFLECTION INSULATION

One way to insulate an object is to reflect incoming thermal radiation. This method is used for (e.g.) heat shields and aluminium foil insulation in building envelopes. In the context of buildings, reflectional insulation limits the heat gain from outside of the building envelope or retards the heat loss during the cold season. In the case of a radiation barrier, the reflective surface is placed in an open airspace, while reflective insulation is placed within a closed airspace, e.g. in front of mass insulation. In the ideal case, where full reflection is attained, heat does not enter the reflectional insulation, and hence all radiative heat is kept out of, or inside, the insulated environment (156–159).

2.1.2. LOW CONDUCTIVITY/CONVECTION INSULATION

Insulation materials with low conductivity and/or low convection capture heat but only let it pass at a low rate. These types of insulation materials enable thermal energy to be kept within a building in cold climates, and outside of the buildings in warmer climates (157). These types of insulation materials primarily remove the contribution from convection and conduction, but also decrease radiative heat transfer. There are different methods of achieving this goal, distinguished by the different ways in which the contributions are limited; i) thermal mass ii) shape or iii) material composition. (156,160)

2.2. INSULATION MATERIAL THEORY

Regardless of the above presented categories of insulation materials, different factors govern the thermal conductivity. The thermal conductivity, λ, describes the migration of thermal energy along a gradient (161), and is the result of several individual contributions (162):

$$\lambda_{total} = \sum \lambda_i, \tag{2.2.1}$$

where solid and gas conduction, convection, radiation and coupling between these are the main contributing elements in insulation materials without free liquid (154). These contributions are all governed by different equations and are generally dependent on temperature.

2.2.1. CONDUCTION

The conduction of heat through a solid phase depends on the vibrations within the atomic lattice and the movement of the electrons. For metals, the movement of the electrons, often denoted as an electron sea, is dominant. The Wiedemann-Franz law describes this by

$$\lambda_{conduction,metal} = L \cdot \sigma \cdot T, \tag{2.2.2}$$

where L is the Lorenz number, T is the temperature and σ is the electric conductivity (151). For materials without free electrons, the conduction of the lattice is dominant instead, and can be written as

$$\lambda_{conduction,lattice} = \lambda_1 + \lambda_2, \tag{2.2.3}$$

where

$$\lambda_1 = \frac{k_B}{2\pi^2 v}\left(\frac{k_B}{\hbar}\right)^3 T^3 \int_0^{\theta_D/T} \tau_c \frac{x^4 e^x}{(e^x-1)^2} dx \tag{2.2.4}$$

and

$$\lambda_2 = \frac{k_B}{2\pi^2 v}\left(\frac{k_B}{\hbar}\right)^3 T^3 \frac{\left(\int_0^{\theta_D/T} \frac{\tau_c \quad x^4 e^x}{\tau_N (e^x-1)^2} dx\right)^2}{\int_0^{\theta_D/T} \frac{\tau_c \quad x^4 e^x}{\tau_N \tau_q (e^x-1)^2} dx}. \qquad 2.2.5$$

k_B is the Boltzman constant, v is the phonon velocity, $\hbar$ is the Planck constant, T is the absolute temperature, θ_D is the Debye temperature for phonons in the given crystal, τ_q is the phonon scattering relaxation time, τ_N is the relaxation time for the so-called "normal processes" and τ_c is the combined relaxation time. For materials with low purity it applies that $\tau_c \approx \tau_q$, and hence $\lambda_1 >> \lambda_2$ (162).

The thermal conductivity for a gas approximates to the ideal gas, and can be described as

$$\lambda_{conduction,gas} = C \cdot v \cdot l, \qquad 2.2.6$$

where C is the heat capacity per unit volume of the gas, v is the average particle velocity and l is the mean free path of the particles (151).

The lower density drives the convection process due to the expansion of heated liquids and gasses. The mass flux is governed by the equation

$$\partial_t \rho = -\partial_j (\rho v), \qquad 2.2.7$$

where the left side represents the time derivative of the density, and the right is the change in mass flux. As the density decreases with increased temperature, this gives rise to mass flow (5). Hence, the resistance to flow within the medium is a governing factor for convection. Darcy's law governs the transport of a fluid through a porous medium:

$$Q = \frac{kA\Delta P}{\mu L}, \qquad 2.2.9$$

where Q is the volume flow, k is the gas permeability, A is the surface area of the flow channel, ΔP is the pressure difference, μ is the fluid viscosity, and L is the length of the flow channel (5).

The airflow can either be obtained directly or as flow velocity. It is noted that the flow velocity is $v = Q/A$.

The permeability of a given material matrix can be described as the fluid conductance of the given, porous material, where a higher pressure difference leads to a higher flowrate. This can be assumed to be linear at low flowrates, but is known to become non-linear at higher flowrates, following the equation

$$\frac{\Delta P}{L} = \frac{\mu \cdot v}{k_1} + \frac{\rho \cdot v^2}{k_2}, \qquad 2.2.10$$

where k_1 is the Darcian permeability, k_2 is the non-Darcian permeability, and ρ is the fluid density (163). It is seen that, at higher viscosities, the impact of the non-Darcian viscosity becomes more dominant. Furthermore, it is known from the literature that these parameters generally increase with the porosity, going towards the value for non-restricted paths (163).

Thermal radiation follows Stefan's law:

$$\lambda_{radiation} = \frac{16}{3}\eta^2 \frac{\sigma}{k_r} T^3, \qquad 2.2.8$$

where η is the refractive index, σ is the Stefan-Boltzmann constant, k_r is the Rosseland mean absorption coefficient and T again is the temperature. The coupling between different, temperature-dependent, heat transfer characteristics can enhance or decrease the thermal conductivity of the bulk material. This can both happen in significant amounts within low-density materials like foams and aerogels with radiation shields, or in materials with point-contacts between fibres and particles. (164)

In total, it is seen that several contributions add up to the total thermal conductivity of porous insulation material. Hence, it is essential to ensure that a total minimum thermal conductivity is reached, rather than one for a single contribution.

2.3. CONVENTIONAL INSULATION MATERIALS

Conventional insulation materials can be found in several forms and combinations thereof are available as commercial solutions. The principal of these forms has different advantages and disadvantages and are briefly discussed below.

2.3.1. FOILS

Thin foils, most often aluminium, can be applied to work as reflectional insulation. As the foil has a high thermal conductivity, it does not prevent heat to be conducted through the foil. These types of foils are often combined with other types of insulation materials, in order to decrease heat conduction through the film (157–159).

2.3.2. BOARDS

Insulation boards of (e.g.) expanded polystyrene or polyurethane foams are used as low thermal conductivity insulation elements. Their structural stability allows them to be placed below layers of concrete without the need of further membranes. These insulation materials are used in several types of buildings due to a combination of low cost and comparatively high thermal conductivity. However, the poor flame-retardant

properties of polymer based materials has to be dealt with. These materials reach thermal conductivities as low as 25 mW/m•K (154,156).

Several mineral-based materials are available as well (165). They exist in both forms, as large boards/slabs, or bricks. They can typically withstand very high temperatures (up to 1050 °C), have a thermal conductivity as low as 80 mW/m•K (166), and are mainly used in furnaces.

2.3.3. LOOSE-FILL

Loose-fill insulation, which can be blown into cavities in the building envelope, is another possibility, especially well-suited for energy renovation of building. Existing hollow walls can be filled by blowing insulation material in. Furthermore, in new buildings with built-in channels funnel the loose-fill insulation throughout the building envelope, thereby making it a cost-effective insulation material (167).

On the microlevel, loose-fill insulation can be made from several materials, including foamed polymer, cellulose, stone, and glass fibres. These materials are transported pneumatically into the building envelope, and offer thermal conductivities as low as 30 mW/m•K (156,167).

2.3.4. FIBRES

Fibre insulation is constructed as mats of varying stiffness, enabling them to be used below layers of concrete and for flexible pipe insulations. The fibres can be created from inorganic materials like glass and stone, as well as from cellulose and wool. These materials can have thermal conductivities as low as 30 mW/m•K (154,156,168–172). The application of inorganic fibre materials is often preferred, due to the inherent high flame retardation properties. Many inorganic materials have low moisture sorption, and are able to dry up efficiently after being soaked (168,171,172).

2.4. NEW MATERIALS

2.4.1. AEROGEL

Several nano porous materials have been investigated as insulation material. Most notably, aerogels with thermal conductivities below 13 mW/m•K, have been developed for advanced applications and are increasingly used for both textile and housing insulation (173,174). Furthermore, aerogel can be highly transparent, and can be applied within windows to enhance the thermal insulation of glass facades (175).

A typical aerogel synthesis is through sol-gel processing followed by supercritical drying. The drying process results in no or low shrinkage (144,174,176). Other types

of gels, like xerogels, are dried by sublimation (144). The gel can either be synthesized in bulk, or 3D-printed by focused laser gelation, resulting in adapted structures down to the micron level (177). The micro-porosity of the aerogel enables the Knudsen-effect, where the air trapped in the material is not able to move by convection. Hence, the thermal conductivity is the only conduction in both gaseous and solid phase, leading to a very low thermal conductivity, and even lower in vacuum (174,178,179).

Aerogels can be composed of several materials, including silica, metal oxides and polymers. They differ in their electric conductivity (180,181), high surface area (143,177,180,182) and thermal insulation properties (178,179). Silica aerogel has the lowest thermal conductivity of these materials (147,174), but in turn is very brittle (143). This makes silica aerogel blocks not well suited for buildings, as vibrations and other movements make them crack up and collapse, when used in a hollow wall (147,150,183). Furthermore, some types are even moisture sensitive, and hence need additional ambient protection (147). Silica aerogel is also available as a powder, but the powder is very fine grained and therefore easily scattered (184). Such a powder is shown in Figure 2-1.

An advantage of polymer aerogels compared to inorganic aerogels are their elastic properties (185). This flexibility allows for incorporation into geometric shapes where the rigid and brittle types are nonapplicable. Their thermal conductivities are as low as 14 mW/m•K. Typical materials are cellulose (150), polyurethane (176) and polyimide (186).

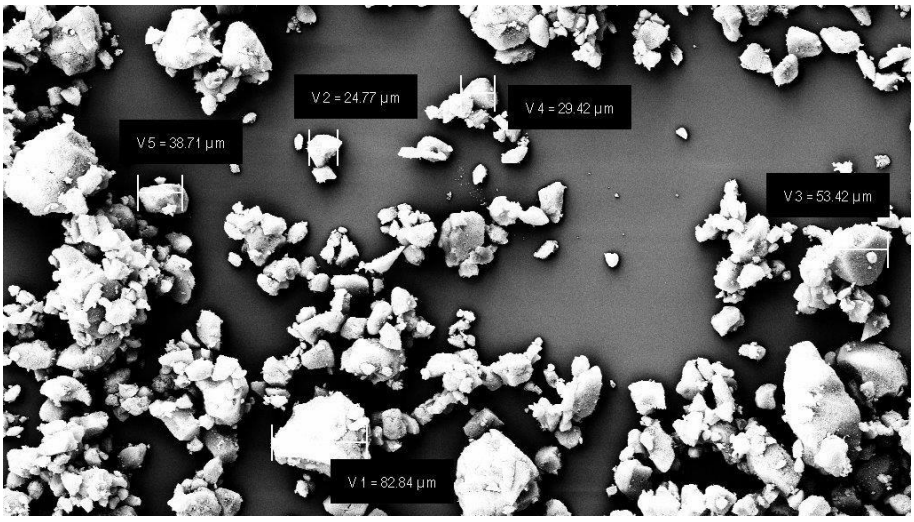

Figure 2-1 – Typical aerogel particles as used during this project, in" Paper 2: Electrospinning of nonwoven aerogel-polyethylene terephthalate composite fiber mats by pneumatic transport" (59)and the non-published article described in Paper 4: Resume of unpublished paper "Melt electrospinning of PET AND PET-aerogel fibres: An experimental and modelling study".

2.4.2. GLASS FOAM

Another non-flammable type of insulation is foam from recycled glass. As the glass is melted under pressure and cast into bricks, it creates a rigid glass foam brick which can be used in similar ways as conventional bricks and porous mineral bricks. These bricks have been created with thermal conductivities as low as 37 mW/m•K and densities of 131 kg/m^3, and they do not only substitute traditional insulation materials but can also be used as structural element as well (187–190).

Different additives, such as MgO_2 and fly-ash, integrated into the glass matrix can further decrease the thermal conductivity. The least thermal conductivity achievable with foamed glass is reached by adding recycled cathode ray tube panel glass. Furthermore, the recycling of glass wastes increases the environmental benefit of this type of insulation material. (187–190)

2.5. COMBINATORIAL MATERIALS

Most materials offer different advantages and drawbacks. To avoid the drawbacks from these materials, combinatorial materials can be created to gain advantages of more than one type of material.

2.5.1. CONCRETE COMPOSITES

The addition of aerogel to concrete can decrease its thermal conductivity, while maintaining the structural strength of the material. The thermal conductivity is decreased by a factor of six, when the aerogel content reaches 80 %vol. However, the compressive strength is decreased by a factor of 30 at the same time. At 50 %vol aerogel content, the thermal conductivity can be decreased by a factor of four, while only decreasing the structural strength by a factor of four. This makes the 50%vol composite material applicable for building applications (191).

2.5.2. REINFORCED DRIED GELS

Aerogels can be reinforced in several ways, including the embedding of electrospun polymer fibres into the aerogel matrix as described above. This reinforcement can be done in several other ways, by either using glass wool (183), polysulphone fibres (183), nanocrystalline cellulose (192) and also carbon nanofibers (193).

2.5.3. VACUUM PANELS

Vacuum insulation panels consist of a fumed silica or aerogel core wrapped in a multilayer airtight metal-polymer foil bag as reflective insulation. Reduced air pressure is applied in order to lower conduction and convection caused by gasses (154,178,179,194–197).

Vacuum insulation panels can have a thermal conductivity in the low range of 4 mW/m•K (195), which makes them suitable for building insulation. Furthermore, the core material is non-flammable, and hence can be used in places where fire protection is vital (154,194,195). The thermal conductivity however can be easily compromised, as puncture, leakage or adsorption of water vapour increases the thermal conductivity of the panel. These panels are not easily replaceable, thus life-span is of huge concern (178).

The performance of the core material, being either aerogel or fumed silica, can be improved by the incorporation of materials blocking the adsorption of water vapour and gasses (194,195). Along the same line, materials which limits the transparency of the core material for IR-radiation will reduce the radiative transport down to 1 mW/m•K (197). All three types of materials can be added inside the protective envelope. Furthermore, the core material can still be brittle, and hence needs reinforcements (178).

CHAPTER 3. RESEARCH PAPERS

In the following section, the research papers published within this PhD project, all with the author of this thesis as primary author and Peter Fojan as senior author, are reprinted. The paper “Solution Electrospinning of Particle-Polymer composite fibres” is published under the creative commons attribution license, and the latter two are licensed by SAGE publishing (198).

The first paper describes the electrospinning of aerogel-polymer solutions into composite fibres with high aerogel contents (198). The second paper covers the same area, but also the introduction of airborne aerogel into the fibre core, and the mechanical properties of the resulting fibres (59). Heat flow in fibre materials is examined in the third paper, which describes the general thermal transport properties of materials akin to those produced in paper one, two and four (199). The fourth paper concerns melt electrospinning with aerogel transported into the fibre core by airflow. This paper is still under review, and hence included as a resume.

The first paper offers insights into fibre morphology, and the influence of aerogel contents on the fibre morphology. The second paper discusses micromechanical phenomena and ways to evaluate the aerogel content of the composite fibres produced by pneumatic aerogel transport. The third paper explores the wettability and gas permeability of meltspun fibres. The fourth paper proposes a model for the polymer viscosity in relation to the melt electrospinning process.

In total, the common denominator of the scientific output of this PhD project is different production and characterization methods for electrospun polymer-aerogel composite fibres.

3.1. PAPER 1: SOLUTION ELECTROSPINNING OF PARTICLE-POLYMER COMPOSITE FIBRES

Manufacturing Rev. 2016, 3, 21
© L. Christiansen and P. Fojan, Published by EDP Sciences, 2016
DOI: 10.1051/mfreview/2016013

Manufacturing Review

Available online at:
http://mfr.edp-open.org

RESEARCH ARTICLE OPEN ACCESS

Solution electrospinning of particle-polymer composite fibres

Lasse Christiansen* and Peter Fojan

Department of Physics and Nanotechnology, Aalborg University, Skjernvej 4, 9220 Aalborg E, Denmark

Received 30 May 2016 / Accepted 15 July 2016

Abstract – Electrospinning is a fast, simple way to produce nano/microfibers, resulting in porous mats with a high surface to volume ratio. Another material with high surface to volume ratio is aerogel. A drawback of aerogels is its inherent mechanical weakness. To counteract this, aerogels can be embedded into scaffolds. The formation of a particle/polymer composite results in improved mechanical stability, without compromising the porosity. In the presented study, aerogel and poly(ethylene oxide) are mixed into a solution, and spun to thin fibres. Thereby a porous membrane, on the micro- and nano-scale, is produced. The maximum polymer-silica weight-ratio yielding stable fibres has also been determined. The morphology of the fibres at different weight ratios has been investigated by optical microscopy and scanning electron microscope (SEM). Low aerogel concentrations yield few particles located in polymer fibres, whereas higher amounts resulted in fibres dominated by the aerogel particle diameters. The diameters of these fibres were in the range between 13 um to 41 um. The flowrate dependence of the fibre diameter was evaluated for polymer solutions with high particle contents. The self-supporting abilities of these fibres are discussed. It is concluded that selfsupporting polymer/aerogel composites can be made by electrospinning.

Key words: Electrospinning, Composite fibres, Poly(ethylene oxide), Aerogel particles

1. Introduction

Electrospinning is an old technique gaining new interest with the increase in nano sized materials. Therefore it becomes an attractive method to produce nanometre sized fibres in a fast and reproducible way [1]. The fibres can be produced from polymer solutions or melts, by placing a polymer droplet into a high electrostatic field. Once the Coulomb attraction overcomes the surface tension, a thin fibre is formed at the tip of the droplet [2]. There after the fibre will be stretched thinner during the migration process towards the collector plate [3]. Fibre diameters have been reported down to a lower limit of 10 nm [4]. The thin fibres are collected as a chaotic fibre mat. This mat, which is porous, can reach surface areas up to 1,000 m^2/g, and has been used as porous membranes in the filter industry [5]. In recent years, electrospun polymer fibres have been used for scaffolding for e.g. biological tissue [6] or for particles [7]. Nano particles have been added for biomedical [8] or energy storage [9] applications, but also micro particles, which were linked together by polymer fibres [10].

Silica aerogel is a type of porous nanomaterial, characterised by its high porosity and extremely low density [11]. The typical formation of aerogels is through solution polymerisation of silica precursors with subsequent solvent exchange followed by supercritical drying [12]. Silica aerogel particles are very brittle, with a typical Young's modulus in the range of 1–10 MPa [13]. For applications where they are subject to load, the introduction of a polymer, and hence the creation of a composite material, will lead to an increase in Young's modulus. Several porous silica composites have been produced. Clay and epoxy in a silica aerogel matrix have been produced, where the gel exhibit elastomeric behaviour [11]. Furthermore, aerogel/polymer microfiber mats can be made by mixing aerogel precursors and microfibers in a mould [14].

The incorporation of small particles, fibres or plates into a composite material can improve its properties. Examples hereof are aluminium metal composites [15], ceramics [16] or epoxy polymer composites [17]. A composite between aerogel and polymer can be used to combine the properties of the flexible polymers and the highly porous but brittle aerogels. Immobilisation of aerogel particles in a fibre matrix combines the properties of both materials forming a composite material with improved mechanical properties of the aerogel. Composites with particles in electrospun fibres have been made [10, 18]. This has been achieved by polymer-particle solution electrospinning [18] as well as core-shell spinning where the particles have been added to the core of the polymer fibre [19].

*Corresponding author: lc@nano.aau.dk

In the present study, a novel approach to incorporate silica aerogel particles into polymer fibre scaffolds is presented. Furthermore the upper limit for the silica content in solution with respect to fibre formation, and the fibre morphology at different polymer/silica ratios, has been investigated in detail.

2. Materials and methods

2.1. Materials

Porous silica particles were supplied by Svenska Aerogel. The particles are hydrophilic and have an average diameter of 14 um. Poly(ethylene oxide) (PEO), with a molecular weight of 900.000 was bought from Sigma Aldrich. Furthermore 99.9% ethanol supplied from VWR Chemicals was used as a solvent. All chemicals were used without further purification.

2.2. Experimental procedure

Polymer solutions were prepared as follows: polymer and silica particles were added into a beaker and gently mixed. First the desired amount of ethanol, followed by deionised water was added under stirring. Typically solutions contained 1.5 g polymer, 30 mL ethanol and 30 mL demineralised water. A varying amount of silica aerogel particles was added, to form 1:1 (w/w) up to 1:9 (w/w) ratio solutions with respect to the polymer. After addition of water, the solutions were placed in a 40 kHz ultrasonic bath for an hour to ensure homogeneous polymer/particle distribution. The solution was stirred overnight.

Electrospinning was performed on an electrospinning setup from Y-Flow. The electrospinning setup has a needle mounted on a moving X-Y stage. The polymer solution is fed from a syringe pump, controlling the flowrate, and high voltage is attached to the spinning needle. The inner diameter of the needle in the spinneret was 0.8 mm. The relative humidity of the electrospinning encasing was kept at 20% via the environmental control system of the setup. For the electrospinning, the needle collector distance was kept at a constant 15 cm. The applied voltage to the needle was 9 kV, and the flowrate was 1.0 mL/h. Microscope glass slides and silicon wafer substrates (1.5 × 1.5 cm) were placed on the collector plate, for sample collection.

Furthermore, for the solution with the highest aerogel particle concentration, resulting in stable fibre formation, the flowrate was varied between 0.25 mL/h and 2.00 mL/h. These samples were further characterised with scanning electron microscopy (SEM).

2.3. Characterisation

The viscosity of the spinning solutions was measured using a Brookfield DV-E rotary viscometer. A 16 mL sample was added to a cavity with a rotating cylinder. The angular velocity was set to 0.3 rpm to determine the viscosity.

After electrospinning, the produced samples were characterised with optical microscopy. Representative overview images were acquired and the morphology of the fibre network was analysed.

SEM was performed on fibres with the highest particle content. A layer of 10 nm gold was deposited on the sample surface by plasma vapour deposition. This was done to ensure conductivity of the sample surface, and prevent charging of the structure during the imaging process. Images were acquired with a Zeiss EVO 60 SEM. The average diameter of each sample was found through analysis with ImageJ. Ten measurements were performed on each fibre batch produced from the flowrate experiments.

Table 1. Solution numbers, weight rations and spinability for different polymer/silica particle ratios.

Solution number	Ratio w/w	Spinability
1	1:1	✓
2	1:2	✓
3	1:4	✓
4	1:6	✓
5	1:8	✓
6	1:9	–

Table 2. Flowrate, average diameter and standard deviation of fibres spun from Solution 5.

Flowrate (mL/h)	Average diameter (um)	Standard deviation (um)
0.25	13.4	4.3
0.50	18.1	4.6
1.00	21.9	7.1
1.50	36.4	6.6
2.00	41.1	15.2

3. Results and discussion

3.1. Spinning solutions and electrospinning

Six solutions were created according to the above described procedure. Their weight ratios between polymer and silica aerogel particles were 1:1, 1:2, 1:4, 1:6, 1:8 and 1:9. They are referred to here as Solution 1–6, and an overview of the numbers, ratios and their respective spinability is summarized in Table 1.

The viscosity of Solution 1 and 6 was measured to 1.38 kCPS and 1.55 kCPS, respectively. The electrospinning of the six solutions was done according to the protocol in Section 2. The flowrate was 1 mL/h for the initial spinning of all six solutions, which all were able to form a Taylor cone with the same electrical field applied. It implies that the amount of silica aerogel particles is of minor importance with respect to Taylor cone formation. However, for Solution 6, no stable fibres have been acquired. It is observed that the minor difference in viscosity did not have any significant effect on the Taylor cone formation and the fibre formation.

Solution 5 proved to be the solution with the highest silica aerogel content, but still yielding stable fibres. With this solution an additional set of experiments was performed in order to investigate the relation between morphology and flowrate. During these experiments the flowrate was varied between

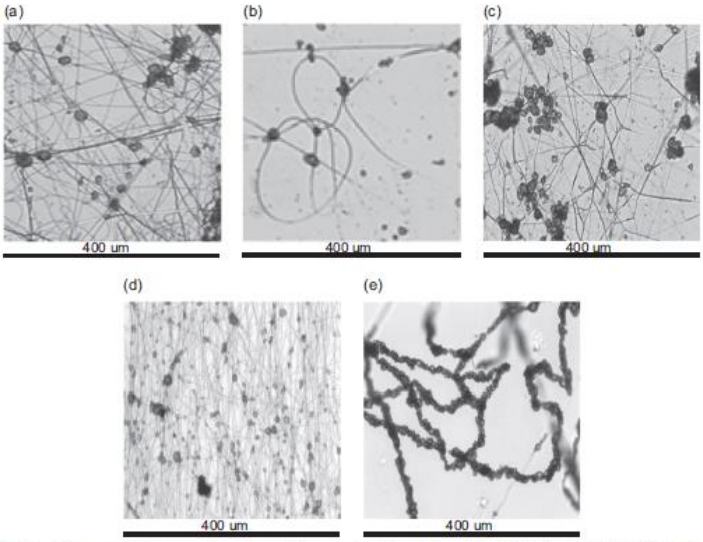

Figure 1. Optical microscopy of fibres spun from polymer/silica aerogel particle solutions with weight rations (a) 1:1, (b) 1:2, (c) 1:4, (d) 1:6 and (e) 1:8. It is seen that the amount of particles increases until the silica aerogel particles packs closely in the fibre.

0.25 mL/h and 2 mL/h. The average diameter of the fibres can be seen in Table 2.

3.2. Optical microscopy

All samples were investigated by optical microscopy. In Figure 1, microscopy images of electrospun fibres from Solution 1–5 are presented (Figures 1a–1e). The fibres with Solution number 1–4 (Figures 1a–1d) all have a pearl-chain shape, where a particle was located in the fibre, with some distance of thin polymer fibre in between the separated particles. The length of polymer fibre between the particles tends to drop with increased particle concentration in the spinning solution. It is also observed that particle aggregates are located inside the fibre matrix, where several aerogel particles stick together.

It is seen that the fibre morphology changes drastically from Solution 4 to 5. By electrospinning the solution, fibres containing closely packed particles are formed. The particles are enveloped in polymer, and stick together. These fibres are the dominant species. This is a change from Solution 1 to 4, where particles are located in the fibre with thin polymer fibre spacing in between. This change can be attributed to a very low amount of polymer available to form fibres. Instead, the silica aerogel particles touch each other, and pack the particles closely in the fibre.

Even though particles are more dominant by weight in all solutions, except Solution 1, the polymer fibre is still the dominant species in the microscopy images. This is due to the relatively low amount of polymer used to create a thin fibre, with diameters in the nanometre range. The particles, on the other hand, are spherical and generally have a much larger diameter than the fibres. For Solution 5, the amount of particles becomes too high that fibres between the particles can be formed. Instead, the polymer glues the silica aerogel particles together.

3.3. Scanning electron microscopy

The fibres spun from Solution 5 were analysed with SEM to obtain more detailed information on the fibre morphology. Solution 5 fibres were spun at flow rates ranging from 0.25 mL/min to 2 mL/min. With increased flowrates, the fibre diameter seemed to increase. This corresponds with the general electrospinning theory of polymer solutions [4]. These fibres are presented in Figure 2. It is seen that thin polymer fibres are still present, but fibres with closely packed particles are the dominant species. The fibres with closely packed particles

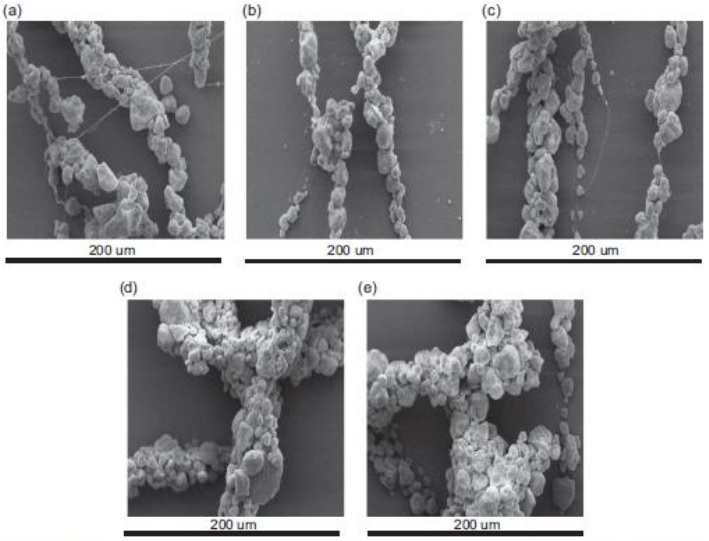

Figure 2. SEM images of fibres spun from Solution 5 with polymer/particle weight ratio 1:8. They are spun at different flowrates: (a) 0.25 mL/h, (b) 0.50 mL/h, (c) 1.00 mL/h, (d) 1.50 mL/h and (e) 2 mL/h. It is seen that higher flowrates in general promoted thicker fibres. All images are 200 um × 200 um.

produced with the same flowrate had a diameter variation of 4–15 um. This can be caused by the turbulent whipping motion where the non-deformable silica aerogel particles have to be held together by the polymer, and hence only the contact surfaces are able to bend.

An in depth analysis of the fibre morphology is presented in Figure 3. The silica aerogel particles are enveloped in polymer and linked together by polymer fibres. The polymer fibres between the particles have diameters between 500 and 800 nm, while polymer fibres not connecting particles had diameters between 200 and 300 nm. This difference can be explained by the increased stretching of the fibres located between particles.

3.4. Fibre characteristics and the influence of silica content

Solution 1–5 produced stable polymer/particle composite fibres. When spun for a longer time period, fibre mats were formed. When spun in a single line over a prolonged period of time, Solution 5 formed a 3D structure, which was strong enough to sustain its own weight. Since Solution 5 contained the highest amount of silica aerogel particles and all the prior analysis of the fibres showed a densely packed particle structure in those fibres, it can be concluded that self-supporting composite fibres containing silica aerogel particles can be created, through embedding them into a fibre matrix. Hence, the method has proven to embed silica aerogel particles into a solid polymer fibre matrix, able to support itself. The self-supporting particle/polymer fibres are presented in Figure 4. The self-supporting fibres have been electro-spun with a line needle movement of 10 mm/s, and a flowrate of 2 mL/h.

Electrospinning of Solution 6 did not produce stable fibres. Instead, a polymer/particle powder was obtained. The particle concentration was too high for the polymer to hold the silica aerogel particles together, and was therefore not forming stable fibres. Hence, this high concentration of silica aerogel particles could not be held together efficiently by the polymer, which in turn did not provide the desired scaffolding for the particles.

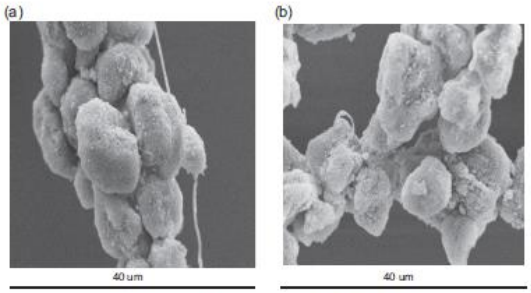

Figure 3. Close-up images of fibres spun from Solution 5. It is seen that the polymer fibres are located among the silica aerogel particles. The images are 40 × 40 um.

Figure 4. Solution 5 electrospun with a 1D needle movement. The structure is seen to be self-supporting.

4. Conclusion

Polymer/silica aerogel particle composite fibres have been produced with polymer/particle weight ratios from 1:1 to 1:8. Increasing particle ratios resulted in increased amounts of particles in a polymer fibre matrix, for Solution 1–4, with silica aerogel/polymer ratios from 1:1 to 1:6. For the solution with a silica aerogel/polymer ratio 1:8, the morphology of the fibres changed from thin polymer fibres supporting particles, to closely packed particles in fibres held together by polymer. For this solution, the flow rate has varied between 0.25 mL/h and 2 mL/h to investigate the influence of flowrate on the fibre morphology. These experiments showed that the fibre diameter increased with flowrate.

Furthermore electrospinning of an aerogel solution with a polymer/particle weight ratio of 1:9 w/w, was also attempted, but did not produce stable fibres. The maximum achievable aerogel/polymer ratio resulting in stable fibres has been found to be 1:8.

5. Implications and influences

This article delivers insight into the topic of production of particle composites by electrospinning. This can be useful for scaffolding of silica aerogel particles of sizes larger than the normal fibre diameter. With increased particle content, it is possible to obtain a structure, where the particles are closely packed in the fibres. Furthermore, if the particle/polymer ratio exceeds an upper limit, no stable fibres can be formed.

Acknowledgements. This project has been financially supported by The Danish Board of Innovation, with funding number J. No. 0052-2012-3.

References

1. C.V. Boys, On the production, properties, and some suggested uses of the finest threads, Proc. Phys. Soc. 9 (1887) 8–19.
2. D. Li, Y. Xia, Electrospinning of nanofibers: reinventing the wheel? Adv. Mat. 16 (2004) 1151–1170.
3. E.H. Shin, K.S. Cho, M.H. Seo, H. Kim, Determination of electrospun fiber diameter distributions using image analysis processing, Macromol. Res. 16 (2008) 314–319.
4. S.V. Fridrikh, J.H. Yu, M.P. Brenner, G.C. Rutledge, Controlling the fiber diameter during electrospinning, Phys. Rev. Lett. 90 (2003) 1445021–1445024.

5. P. Gibson, H. Schreuder-Gibson, D. Rivin, Transport properties of porous membranes based on electrospun nanofibers, Colloids Surf. Physicochem. Eng. Asp. 187 (2001) 469–481.
6. H. Yoshimoto, Y.M. Shin, H. Terai, J.P. Vacanti, A biodegradable nanofiber scaffold by electrospinning and its potential for bone tissue engineering, Biomaterials 24 (2003) 2077–2082.
7. X.-J. Han, Z.-M. Huang, C. Huang, Z.-F. Du, H. Wang, J. Wang, C.-L. He, Q.-S. Wu, Preparation and characterization of electrospun polyurethane/inorganic-particles nanofibers, Polym. Compos. 33 (2012) 2045–2057.
8. T. Hasell, K.J. Thurecht, R.D. Jones, P.D. Brown, S.M. Howdle, Novel one pot synthesis of silver nanoparticle – polymer composites by supercritical CO_2 polymerisation in the presence of a RAFT agent, Chem. Commun. 31 (2007) 3933–3935.
9. L. Ji, X. Zhang, Electrospun carbon nanofibers containing silicon particles as an energy-storage medium, Carbon 47 (2009) 3219–3226.
10. T. Ding, Y. Tian, L. Kui, K. Clays, K. Song, Y. Guoqiang, C.-H. Tung, Anisotropic oxygen plasma etching of colloidal particles in electrospun fibers, Chem. Commun. 47 (2011) 2429–2431.
11. E.M. Arndt, M.D. Gawryla, D.A. Schiraldi, Elastic, low density epoxy/clay aerogel composites, J. Mater. Chem. 17 (2007) 3525–3529.
12. J. Biener, M. Stadermann, M. Suss, M.A. Worsley, M.M. Biener, K.A. Rose, T.F. Baumann, Advanced carbon aerogels for energy applications, Energy Environ. Sci. 4 (2011) 656–667.
13. T. Woignier, J. Phalippou, H. Hdach, G. Larnac, F. Pernot, G.W. Scherer, Evolution of mechanical properties during the alcogel-aerogel-glass process, J. Non-Cryst. Solids 147 (1992) 672–680.
14. C.J. Stepanian, G.L. Gould, R. Begag, Patent US7078359 – Aerogel composite with fibrous batting, US7078359 B2, 2006.
15. A.V. Muley, S. Aravindan, I.P. Singh, Nano and hybrid aluminum based metal matrix composites: an overview, Manufacturing Rev. 2 (2015) 15.
16. T. Ohji, Y.-K. Jeong, Y.-H. Choa, K. Niihara, Strengthening and toughening mechanisms of ceramic nanocomposites, J. Am. Ceram. Soc. 81 (1998) 1453–1460.
17. S. Varghese, J. Karger-Kocsis, Natural rubber-based nanocomposites by latex compounding with layered silicates, Polymer 44 (2003) 4921–4927.
18. M.M. Demir, M.A. Gulgun, Y.Z. Menceloglu, B. Erman, S.S. Abramchuk, E.E. Makhaeva, A.R. Khokhlov, V.G. Matveeva, M.G. Sulman, Palladium nanoparticles by electrospinning from poly (acrylonitrile-co-acrylic acid)-$PdCl_2$ solutions. Relations between preparation conditions, particle size, and catalytic activity, Macromolecules 37 (2004) 1787–1792.
19. Y. Yu, L. Gu, C. Wang, A. Dhanabalan, P.A. van Aken, J. Maier, Encapsulation of Sn@ carbon nanoparticles in bamboo-like hollow carbon nanofibers as an anode material in lithium-based batteries, Angew. Chem. Int. Ed. 48 (2009) 6485–6489.

Cite this article as: Christiansen L & Fojan P: Solution electrospinning of particle-polymer composite fibres. Manufacturing Rev. 2016, 3, 21.

3.2. PAPER 2: ELECTROSPINNING OF NONWOVEN AEROGEL-POLYETHYLENE TEREPHTHALATE COMPOSITE FIBER MATS BY PNEUMATIC TRANSPORT

Article

JOURNAL OF COMPOSITE MATERIALS

Journal of Composite Materials
0(0) 1–6

DOI: 10.1177/0021998319829889
journals.sagepub.com/home/jcm
SAGE

Electrospinning of nonwoven aerogel-polyethene terephthalate composite fiber mats by pneumatic transport

Lasse Christiansen, Lars R Jensen and Peter Fojan

Abstract

The use of fiber materials includes construction-, automotive-, textile industry, to filters for water and air cleaning as well as hydroponic growth media. Different applications demand different fiber types and properties. This study presents a new production method for a composite fiber material composed of a dry aerogel particle and a polymer. The production method combines the electrospinning process with pneumatic transport of aerogel particles and creates aerogel–polymer composite fibers. The fibers are characterised through scanning electron microscopy, thermogravimetric analysis and tensile testing. They are compared to reference fibers made of pure polymer. The experiments yielded an aerogel–polymer composite fiber material, which contained aerogel particles. This fiber material did not contain excess solvent, and supported the aerogel particles. The strain to failure and the maximum force per weight were found to be lower for the aerogel–polymer composite fibers compared to reference fibers without aerogel.

Keywords

Electrospinning, aerogel, composite fibers

Introduction

The technique of electrospinning has gained new interest due to the increasing research in nanofibre materials. It is an attractive method since it allows for mass production of nano-sized fibers in a fast and reproducible way.[1] These fibers are produced by placing a droplet of polymer melt or solution in a high electrostatic field. The field induces charge build up in the liquid, and these charges will be subject to a Coulomb force, also due to the field. When the Coulomb force surpasses the surface tension, a thin fiber emerges from the droplet through the formation of a Taylor cone.[2] When the fiber is electrospun from the droplet, the droplet shrinks. In order to maintain a stable Taylor cone, a feed of polymer solution can be applied through a needle, e.g. with a syringe pump,[3] or needleless electrospinning, where the curvature of a droplet enables the Taylor cone formation.[4,5]

The fiber stretches, as it migrates through the electrostatic field, towards the collector,[6] and as the fiber stretches, it also becomes thinner; the lowest fiber diameters produced by electrospinning are down to 10 nm.[7] The fibers can be collected as non-woven fiber mats or as aligned fibers in one direction when different collectors are applied.[8] The fiber mats are porous, and the surface area can reach up to 1000 m^2/g, which makes them applicable as filter materials.[9] These materials have lately also gained interest in regenerative medicine as scaffolds.[10,11]

Silica aerogel is another type of material with high porosity and an extremely low density.[12] Aerogel has surface areas up to 3200 m^2/g,[13] is very brittle and typically has Young's modulus in the range of 1–10 MPa.[14] When aerogel is subject to loads, a polymer can be introduced to increase the strength of the material. This creates a polymer/aerogel composite. Different approaches have been made to produce aerogel/

Department of Materials and Production, Aalborg University, Denmark

Corresponding author:
Peter Fojan, Department of Materials and Production, Aalborg University, Aalborg E 9220, Denmark.
Email: fp@nano.aau.dk

polymer composites,[15–19] including bendable aerogel sheets[20] and vesting of fiber containing aerogel blocks.[21] Another method to maintain a high porosity and surface area, while improving the mechanical properties, could be to incorporate aerogel particles into an electrospun non-woven fiber mat.

When small particles are incorporated into a polymer material, the properties of the material can change. Examples can be rubber/silicate composites,[22] carbon nanotubes/polylactides,[23] ceramic-,[24] or metal composites.[25] When combining aerogel and polymer fibers, the flexible polymer properties could be used to support the highly porous, but brittle, aerogels. Composites of nanoparticles and polymer have been created by both single needle[26] and coaxial electrospinning[27] methods. The incorporation of aerogel particles into a polymer fiber matrix from solution has also been achieved.[28] In these earlier experiments by this group, the aerogel and polymer were suspended in water, and the aerogel was coated in polymer, which leads to closed pores in the aerogel, not contributing to the surface area of the material. For some applications, e.g. gas sensors, this would be a disadvantage.[29]

This work aimed to produce aerogel–polymer composite fibers through electrospinning. We hypothesise that it is possible to produce aerogel–polymer composites by conveying aerogel powder into an electrospinning nozzle by pneumatic transport. We present a method for production of aerogel–polymer fibers, as well as a morphological study of the resulting composite fibers. The final aerogel content of the fibers is evaluated by thermogravimetric analysis, and the load-carrying capabilities of the fibers are evaluated. In the end, the discussion covers the properties, and possible uses of the material.

Materials and methods

Goodfellow supplied polyethene terephthalate (PET). Dichloromethane (DCM) and trifluoroacetic acid (TFA) were purchased from Sigma Aldrich. Aerogel powder was purchased from Insulgel High-Tech Co., Ltd (Beijing, China), with a maximum particle size of 80 nm and a density of 0.008 kg/L.[30] All chemicals were used without further purifications.

Polymer solutions were prepared by dissolving 20% wt. PET in DCM and TFA (7:3 vol/vol). The polymer was stirred overnight, at 60°C on a magnetic stirrer with hot plate (IKA RCT Basic). The solution was electrospun after minimum 24 h.

When aerogel–polymer solutions were prepared, aerogel was added to the solvents before the polymer to provide a homogeneous solution; 4 g of polymer was added to each solution, after 0.25–1.50 g of aerogel. After 24 h of stirring, the polymer solution appeared as a homogeneous solution.

Electrospinning was performed in an inverted configuration by applying a high voltage to the collector and ground to the needle. Yflow S.D., (Malaga, Spain) sold the equipment. The needle, both single and coaxial, Figure 1, was mounted on an x-y stage.

A syringe pump provided polymer flow at a constant feed rate. For the fibers produced with coaxial spinning, aerogel was transported into the needle core pneumatically, by dry nitrogen flow. Figure 2 shows a sketch of the setups.

The experiments included three different sets of fibers: Reference fibers without aerogel, composite

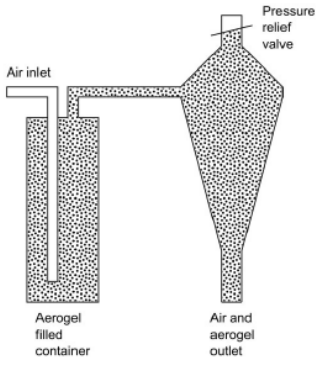

Figure 2. The aerogel inlet system. Nitrogen travels through a rinsing flask filled with aerogel. It is conveyed into a funnel, ending in a piece of tubing, keeping the aerogel nitrogenborne into the spinning needle.

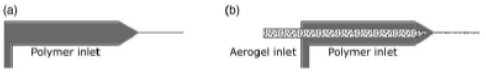

Figure 1. Schematics of (a) single needle and (b) coaxial needle. The inner needle transports aerogel, and the outer one transports polymer solution.

polymer–aerogel fibers from a mixture, and coaxial electrospun fibers with polymer applied in the outer needle and nitrogen-aerogel in the inner. The spinning of the two first fibers types was done through a single needle and the last fibers with a coaxial needle setup.

All three fiber types were electrospun at −16 kV applied to the collector plate. The distance from the needle tip to the collector plate was kept constant at 21 cm. The polymer flow rate was between 1 and 2 ml/h. The nitrogen flow rate for the spinning of the coaxial electrospun fibers was between 0.5 and 2 L/min.

Morphology analysis of the fibers was done with scanning electron microscopy (SEM), using a ZEISS EVO 60. A 10 nm gold layer was deposited by plasma vapour deposition onto the samples before analysis to ensure conductivity.

Thermogravimetric measurements were performed on a Discovery TGA 550 from TA Instruments in air from room temperature to 1000°C. The airflow rate was 10 ml/min, and the heating rate was 20°C/min.

Tensile tests were performed on a TST 350 micro tensile stage from Linkam Scientific at a speed of 30 mm/min. The tests were performed on rectangular samples with a length and width of 30 mm and 10 mm, respectively. The samples were cut using a scalpel.

The force and elongation of the sample were measured during the testing.

Results and discussion

The reference fibers were electrospun from a single needle with a rate of 1 ml/h, and with x-axis movement speed of the needle of 10 mm/s, and y-axis shift of 5 mm, over an area of 200 × 200 mm. The spinning process continued for 12 h, resulting in an electrospun mat useable for mechanical testing. The mass of this mat was 4 g. Figure 3 shows an image of the reference fibers.

Mixture fibers were electrospun through a single needle, to validate the spinnability of a composite consisting of aerogel and polymer. These fibers were electrospun with a flow rate of 1 ml/h, from solutions with aerogel–polymer weight ratios of 0.25:4, 0.50:4, 1.00:4, 1.33:4 and 1.50:4. The aerogel–polymer solutions, with weight ratios 0.25:4, 0.50:4, 1.00:4, and 1.33:4, yielded stable electrospinning. In the case of the aerogel–polymer solution with a weight ratio of 1.50:4, the droplet tended to dry out. Images of fibers obtained from the aerogel–polymer solution, with a weight ratio of 1.33:4, are shown in Figure 4. The aerogel was incorporated in the fiber matrix. The total weight ratio for these fibers was lower than previously shown for other solvents and polymers, as the mixture was not spinnable at higher contents due to the rapid evaporation of the solvent.

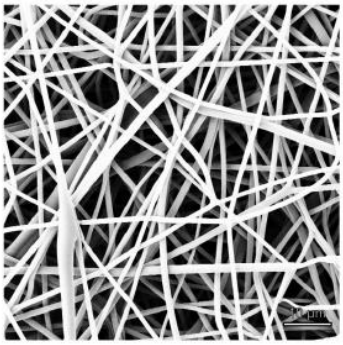

Figure 3. Reference fibers electrospun from PET solution.

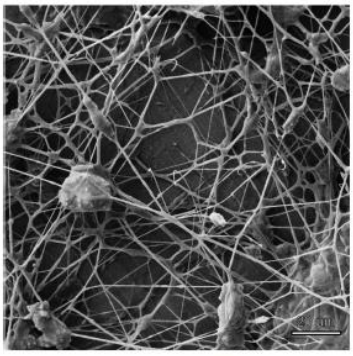

Figure 4. Fibers electrospun from a PET-Aerogel solution with weight ratio 2:1. It is seen that both large and small aerogel particles are present in the fiber network.

The aerogel particles tend to be inside the polymer matrix, and hence small particles are not visible.

For the coaxially electrospun polymer–aerogel fibers, both the feed-rate of the polymer and the airflow through the aerogel system have been optimised and the maximum and minimum values for both parameters, yielding stable electrospinning conditions, have been established. With a polymer flow rate

below 0.5 ml/h, the droplet dried out, and flow rates above 3 ml/h caused dripping of the solution. Airflow rates below 0.5 L/min did not transport enough aerogel to be detected in the fibers. Airflow rates above 2 L/min caused spraying of the polymer solution. Air flow rates between 1.0 to 1.5 L/min provided the most stable conditions. At an airflow rate of 1.0 L/min, least clogging of the needle was observed.

A fiber mat produced with a polymer solution flow rate of 1 ml/h and an aerogel-airflow rate of 1 L/min was obtained for testing. The x-axis velocity of the needle was 10 mm/min; the y-movement step was 5 mm. The fibers were electrospun over an area of 100 × 100 mm. The spinning proceeded continuously, for a total of 10 h. In this time-span, a non-woven fiber mat was produced with a weight of 3.3 g. It was observed that aerogel was not only contained inside the fibers, as excess aerogel was observed in the electrospinning enclosure.

An overview image, together with a close-up image, is shown in Figure 5. From the close-up image, it is evident that the aerogel is located inside the fibers, but on the surface as well. In the overview image, larger particles are seen to stick to the surface of the fibers. The typical fiber diameter is around 1 μm. In this image, it can be observed that the polymer fibers act as a scaffold for the larger aerogel particles. Core-shell fibers were not formed which corresponds to earlier studies.[31] Even though the process did not result in core-shell fibers, the coaxial needle can be used to introduce particles into an electrospun fiber matrix, which would be able to support the aerogel for various applications. Furthermore, this technique does not soak the aerogel with solvent or encapsulates it in the polymer, which might be beneficial for specific applications. These two points are the main advantages of this technique, while the low production rate, as for other single needle electrospinning methods, is the dominant drawback.

TGA measurement curves for the reference fibers and the coaxially spun fibers are shown in Figure 6. It can be observed that both fiber materials show

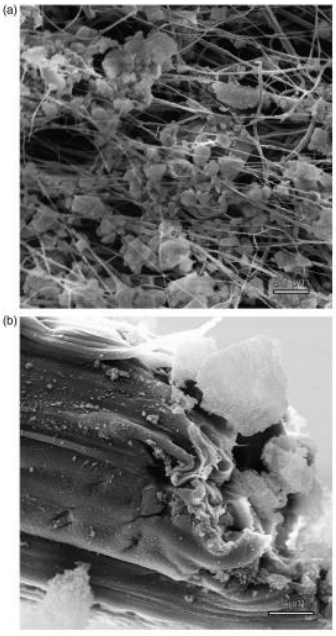

Figure 5. Blow spun fibers with aerogel pneumatically transported into the spinning nozzle. (a) An overview image showing the aerogel distributed in the fiber network and (b) a magnified image of a fiber in cross-section, which shows aerogel is located both inside and outside of the fiber.

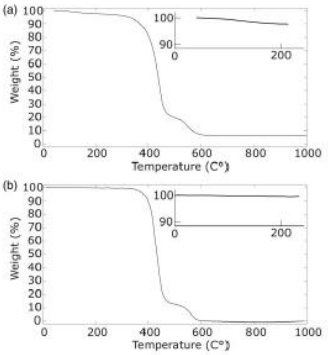

Figure 6. TGA curves for (a) for PET-Aerogel blow spun fibers, and (b) PET reference fibers. The difference between the two curves at 800 °C is 7%, corresponding to the aerogel weight content.

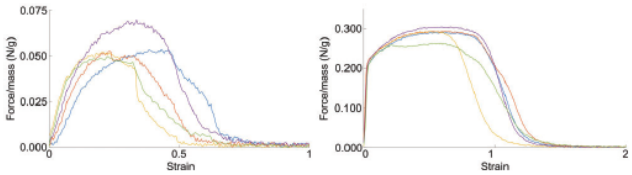

Figure 7. Force per mass as a function of strain: Left) PET-aerogel blow spun fibers and Right) PET reference fibers. It is seen that the composite fibers have a force pr. mass ratio for failure four to five times lower than the reference fibers.

a primary degradation between 400 and 450°C, and a minor, secondary degradation around 525°C, which corresponding well with other studies of PET.[32] For the aerogel-PET fiber material, a mass loss of 3% is observed starting at approximately 100°C. As no mass loss is observed for the reference fibers, this is contributed to the evaporation of water bound to the aerogel. Neither of the samples shows a mass-loss below 100°C indicating that no solvents from the spinning process are present in the fiber material since the boiling points of DCM and TFA are 39°C and 72°C, respectively. By comparing the mass of the fiber materials, at temperatures significantly above the secondary degradation temperature of PET, the amount of aerogel in the composite fibers can be determined. At 800°C, a difference of 7 wt.% is observed between the two fiber materials, and since silica aerogel is thermally stable at this temperature, the entire mass difference is related to the aerogel content in the fibers.

Tensile tests were performed on mats of both reference fibers and aerogel–polymer composite fibers. The force applied to and elongation of the sample was recalculated into force/mass and strain, respectively. Figure 7 shows the resulting curves. Force per mass is calculated in favor of stress due to the fluffiness of the sample making the material thickness not well-defined.

It is observed that the maximum force per weight for the polymer-aerogel samples is between 15% and 23% of the reference fibers. Furthermore, the failure strain of the polymer-aerogel fibers is 50% or less than that of the reference fibers. The significant reduction in force/weight and failure strain of the polymer–aerogel fibers indicates that the aerogel acts as defects in the fibers. On the other hand, this also indicates that the aerogel particles are trapped in a fiber network allowing them to withstand a larger strain to failure than the aerogel itself, which makes them applicable in more fields. Then, the aerogel composite fibers are applicable, where aerogel particles would drift off, and bulk aerogel would be too brittle.

Conclusion

Electrospinning from a coaxial needle produced aerogel–polymer composite fibres. The aerogel has been transported into the inner fiber by pneumatic transport with dry nitrogen as carrier gas.

This production method resulted in coaxial electrospun fibers with aerogel particles trapped both inside the fibers, but also in the fiber network, when the size of the particles exceeded the fiber diameter.

The polymer solution flow rate as well as the nitrogen flow rate were critical parameters to obtain stable electrospinning conditions. Too low polymer flowrates would cause a fast drying at the Taylor cone, and a too high polymer flow rate resulted in dripping. For the nitrogen flow rate, a too low flowrate would not transport aerogel into the inner needle, and a too high flow rate would result in electrospraying instead. This narrow range of parameters limits the production variation and should be considered for the processing of other materials.

Compared to reference fibers (pure PET), the composite fibers exhibited a lower force/weight ratio, and the measured failure strain was less consistent, as the large aerogel particles cause defects in the fiber material. Hence, the fiber material can be used to introduce aerogel into light load applications where neither bulk aerogel, nor aerogel particles are suitable.

Declaration of Conflicting Interests

The author(s) declared no potential conflicts of interest with respect to the research, authorship, and/or publication of this article.

Funding

The author(s) disclosed receipt of the following financial support for the research, authorship, and/or publication of this article: This project has been financially supported by The Danish Board of Innovation, with funding number J.no. 0052-2012-3.

ORCID iD

Lasse Christiansen http://orcid.org/0000-0002-1771-3934

References

1. Boys CV. On the production, properties, and some suggested uses of the finest threads. *Proc Phys Soc* 1887; 9: 8–19.
2. Li D and Xia Y. Electrospinning of nanofibers: reinventing the wheel? *Adv Mater* 2004; 16: 1151–1170.
3. Yang Y, Jia Z, Li Q, et al. A shield ring enhanced equilateral hexagon distributed multi-needle electrospinning spinneret. *IEEE Transac Dielectrics Electric Insul* 2010; 17: 1592–1601.
4. Lu B, Wang Y, Liu Y, et al. Superhigh-throughput needleless electrospinning using a rotary cone as spinneret. *Small* 2010; 6: 1612–1616.
5. Yarin A and Zussman E. Upward needleless electrospinning of multiple nanofibers. *Polymer* 2004; 45: 2977–2980.
6. Shin EH, Cho KS, Seo MH, et al. Determination of electrospun fiber diameter distributions using image analysis processing. *Macromol Res* 2008; 16: 314–319.
7. Merkel TC, Freeman BD, Spontak RJ, et al. Sorption, transport, and structural evidence for enhanced free volume in poly (4-methyl-2-pentyne)/fumed silica nanocomposite membranes. *Chem Mater* 2003; 15: 109–123.
8. Persano L, Camposeo A, Tekmen C, et al. Industrial upscaling of electrospinning and applications of polymer nanofibers: a review. *Macromol Mater Eng* 2013; 298: 504–520.
9. Gibson P, Schreuder-Gibson H and Rivin D. Transport properties of porous membranes based on electrospun nanofibers. *Colloids Surf A* 2001; 187: 469–481.
10. Mendes AC, Stephansen K and Chronakis IS. Electrospinning of food proteins and polysaccharides. *Food Hydrocolloids* 2017; 68: 53–68.
11. Khorshidi S, Solouk A, Mirzadeh H, et al. A review of key challenges of electrospun scaffolds for tissue-engineering applications. *J Tissue Eng Regenerat Med* 2016; 10: 715–738.
12. Ayers MR and Hunt AJ. Molecular oxygen sensors based on photoluminescent silica aerogels. *J Non Crystall Solids* 1998; 225: 343–347.
13. Kabbour H, Baumann TF, Satcher JH, et al. Toward new candidates for hydrogen storage: high-surface-area carbon aerogels. *Chem Mater* 2006; 18: 6085–6087.
14. Woignier T, Phalippou J, Hdach H, et al. Evolution of mechanical properties during the alcogel-aerogel-glass process. *J Non Crystall Solids* 1992; 147: 672–680.
15. Arndt EM, Gawryla MD and Schiraldi DA. Elastic, low density epoxy/clay aerogel composites. *J Mater Chem* 2007; 17: 3525–3529.
16. An H, Wang Y, Wang X, et al. Polypyrrole/carbon aerogel composite materials for supercapacitor. *J Power Sources* 2010; 195: 6964–6969.
17. Li L, Yalcin B, Nguyen BN, et al. Flexible nanofiber-reinforced aerogel (xerogel) synthesis, manufacture, and characterization. *Appl Mater Interf* 2009; 2009: 2491–2501.
18. Salimian S, Zadhoush A, Naeimirad M, et al. A review on aerogel: 3D nanoporous structured fillers in polymer-based nanocomposites. *Polym Compos* 2018; 39: 3383–3408.
19. Krishnaswamy S, Bhattacharyya D, Abhyankar H, et al. Morphological, optical and thermal characterisation of aerogel-epoxy composites for enhanced thermal insulation. *J Compos Mater*. Epub ahead of print 15 August 2018. DOI: 10.1177/0021998318793194.
20. Yeo J-G, Lee E, Cho C-H, et al. *Patent – method for producing sheets including fibrous aerogel*. US8647557, www.google.com/patents/US8647557 (2014, accessed 5 January 2015).
21. Wu H, Chen Y, Chen Q, et al. Synthesis of flexible aerogel composites reinforced with electrospun nanofibers and microparticles for thermal insulation. *J Nanomater* 2013; 2013: 10.
22. Varghese S and Karger-Kocsis J. Natural rubber-based nanocomposites by latex compounding with layered silicates. *Polymer* 2003; 44: 4921–4927.
23. Yang T, Wu D, Lu L, et al. Electrospinning of polylactide and its composites with carbon nanotubes. *Polym Compos* 2011; 32: 1280–1288.
24. Bai Y, Cheng Z-Y, Bharti V, et al. High-dielectric-constant ceramic-powder polymer composites. *Appl Phys Lett* 2000; 76: 3804–3806.
25. Muley AV, Aravindan S and Singh IP. Nano and hybrid aluminum based metal matrix composites: an overview. *Manuf Rev* 2015; 2: 15.
26. Demir MM, Gulgun MA, Menceloglu YZ, et al. Palladium nanoparticles by electrospinning from poly (acrylonitrile-co-acrylic acid)-PdCl2 solutions. Relations between preparation conditions, particle size, and catalytic activity. *Macromolecules* 2004; 37: 1787–1792.
27. Yu Y, Gu L, Wang C, et al. Encapsulation of Sn@ carbon nanoparticles in bamboo-like hollow carbon nanofibers as an anode material in lithium-based batteries. *Angewandte Chem Int Ed* 2009; 48: 6485–6489.
28. Christiansen L and Fojan P. Solution electrospinning of particle-polymer composite fibers. *Manuf Rev* 2016; 3: 1–6.
29. McAleer JF, Moseley PT, Norris JO, et al. Tin dioxide gas sensors. Part 1 – aspects of the surface chemistry revealed by electrical conductance variations. *J Chem Soc Faraday Transac 1* 1987; 83: 1323–1346.
30. Insulgel High-Tech Co. *Insulgel data sheet*. Beijing, China: Author, 2014.
31. Sun Z, Zussman E, Yarin AL, et al. Compound core-shell polymer nanofibers by co-electrospinning. *Adv Mater* 2003; 15: 1929–1932.
32. Cooney JD, Day M and Wiles D. Thermal degradation of poly (ethylene terephthalate): a kinetic analysis of thermogravimetric data. *J Appl Polym Sci* 1983; 28: 2887–2902.

3.3. PAPER 3: HEAT AND AIR TRANSPORT IN DIFFENTLY COMPACTED FIBRE MATERIALS

Article

Journal of Industrial Textiles

0(0) 1–14

DOI: 10.1177/1528083719900386
journals.sagepub.com/home/jit
SAGE

Heat and air transport in differently compacted fibre materials

Lasse Christiansen[1], Yovko Ivanov Antonov[2], Rasmus Lund Jensen[2], Emmanuel Arthur[3], Lis Wollesen de Jonge[3], Per Møldrup[2], Hicham Johra[2] and Peter Fojan[1]

Abstract

Fibre materials are widely used as insulation materials in both clothing and the building industry. The transport of heat and air through fibre insulation materials are accountable for both the energy need for indoor space conditioning and the indoor environment quality inside buildings. A better understanding of the thermodynamics of those materials can enable higher quality products for improved energy efficiency. By using fast gas permeability measurements and more time-consuming guarded hot plate measurements, this study investigates the link between thermal conductivity and gas permeability for Rockwool, Kevlar and polyester fibres, at different compaction levels. Correlations between gas permeability and thermal conductivity at different total volumes of solid are presented. The experimental results show that the gas permeability and thermal conductivity exhibited a change in their evolution trend, due to compaction, in the same zone of the total volume of solid for all materials. The presence of this transition zone enables to establish a link between the measurement of gas permeability and thermal conductivity. This correlation can be employed to perform rapid thermal conductivity assessment of fibrous material, which can be cost-effective for fibre manufacturers or building contractors, but also quality assessment in the textile industry.

[1]Department of Manufacturing and Production, Aalborg University, Aalborg Ø, Denmark
[2]Department of Civil Engineering, Aalborg University, Aalborg Ø, Denmark
[3]Faculty of Science and Technology, Department of Agroecology, Aarhus University, Tjele, Denmark

Corresponding author:
Peter Fojan, Department of Manufacturing and Production, Aalborg University, Skjernvej 4, 9220 Aalborg Ø, Denmark.
Email: fp@mp.aau.dk

Keywords
Fibrous materials, testing, structure-properties, measurement

Introduction

For energy consumption, heat and airflow are essential parameters. The exfiltration of hot air, as well as the internal transport of hot air to cold surfaces, are two of the contributions to heat loss [1]. To decrease heat losses, air transport can be diminished, and the cold surfaces made less thermally conductive. The decrease of thermal conductivity in a material can be obtained in different ways. Solid phase in materials holds the largest share of conductive heat transfer. Replacing this solid phase with trapped air or gas, as in foam materials, or even remove it, like in vacuum insulation panels, is a very efficient way of reducing the thermal conductivity of the material [2].

Fibre materials reduce the movement of air [3]. Woolly fibres from animals as well as plants insulate the host by immobilising the air inside the fibre matrix, while still being permeable to a certain extent [3]. Different applications calls for different properties of fibre materials, e.g. the feeling of comfort of clothing is closely related to thermal effusively [4], while fire fighter protection gear is highly dependent on the heat and moisture transport through the clothing [5,6]. Low thermal conductivity also makes fibre materials suited for use as insulation materials in the building industry [7,8], where they insulate the building envelope and at the same time allow moisture to escape through the fibre network. Hence, fibre materials are commonly used to manufacture insulation elements for the building industry [9]. They insulate by immobilising the air in the fibre structure; convection is minimised, and the limited contact between the fibres reduces conduction [10]. The most common insulation materials employed in the building sector are mineral wool and glass wool [2]. For personal insulation clothing, natural and polymer fibres are often used [3].

The effective thermal conductivity of a material is dependent on the thermal conductivity of each present phase: the natural convection due to temperature gradient, the forced convection due to leakage through open pores, and the coupling between each of the other contributions [2]. Each of these contributions can have different local minima with respect to e.g. total volume content of solids. The overall minimum effective thermal conductivity will then be desirable for insulation material. The mechanics of each of these factors is crucial for the development and application of high-quality insulation fibrous materials.

The choice of raw fibre material for insulation is essential when considering factors affecting heat and air transport processes [1]. The low thermal conductivity of the raw material will decrease the thermal transport by conduction through the solid fibre matrix. If the total volume content of solids falls below a certain threshold, e.g., 0.01 for fibre glass, radiation will become dominant [11]. The convection

process is more dependent on the fibre network structure than on the material choice. However, moisture behaviour will be significantly influenced by choice of raw material [1,10]. A hydrophobic material does not attract or adsorb any water vapour, contrary to a hydrophilic one. Furthermore, some materials only adsorb vapour on the surface, while others can diffuse vapour deeper inside the material matrix and release it when ambient humidity decreases [12,13].

The connection between the solid phases for a given total volume content of solids, and hence the tortuosity of the pore network depends on the attraction between each fibre. For glass particles between 20 µm and 100 µm on a silicon substrate, the attractive forces increase with respect to humidity. The increase is larger above 40% relative humidity, suggesting that liquid bridges start to form [14]. This corresponds to two or three layers of water molecules on the fibre [15]. On the contrary, for relative humidity below 40%, it was observed that the force between certain fibres is sometimes repulsive. This is explained by electrostatic repulsion when no liquid layer has formed on the surface of the fibres [14,16]. In general, the thermal conductivity increases with the increase of moisture content due to the high thermal conductivity of water replacing low thermal conductivity air in the pores, and more contact between the fibres [17]. These effects can be further enhanced, if the binder in e.g. mineral wool is not properly cured. In that case, moisture will increase thermal conductivity and decrease the mechanical strength of the fibre insulation material [18,19].

This paper presents the concept of fibre material characterization by combining thermal and pore-network measurements for both convection-dominated and conduction-dominated cases (Figure 1). In a convection dominated-material, the air phase is responsible for the primary heat transfer. When the material becomes more compact, the increased contact between fibres and the less permeable fibre network results in a conduction-dominated heat transfer. By testing three different fibre materials, this paper demonstrates that a change in both thermal conductivity and gas permeability happens when the materials are compressed towards a higher total volume content of solid. The effect of relative humidity on the fibre behaviour

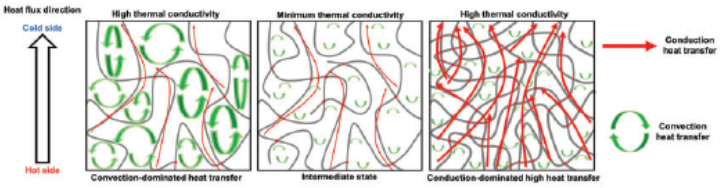

Figure 1. Illustration of two hypothesized states of porosity and pore structure during compression of fibre material. Red arrows represent conduction, green convection. Less compacted and convection dominated pore network (left); higher compaction and conduction-dominated pore network (right). In the middle, an intermediate state where the sum of the two has a minimum thermal conductivity.

is discussed, together with the possibility to use the fast gas permeability measurement as a screening method instead of the more time-consuming thermal conductivity method.

Materials and methods

Three different fibre materials were characterized: Rockwool Flexibat 100™, Kevlar 49™ and electrospun polyethene terephthalate (PET) fibres (see Table 1). The Kevlar fibres and the PET pellets used for electrospinning [20] were bought from Goodfellow (Huntingdon, England) and were used as supplied without any further purification or modification.

The material characteristics were obtained from the following methods (see Figure 2). All three fibre types were examined with scanning electron microscopy (SEM). The fibres were placed on a silicon wafer, and a droplet of ethanol is added to stabilize the position of the fibre on the wafer. As all fibre materials are non-conducting, they were sputter-coated with a 10 nm gold layer by physical vapour deposition prior to observation. This method produces high-resolution microstructure images together with estimates of the fibre diameters.

The equilibrium moisture content for the relative humidity ranges from 3% to 93%. The sorption-desorption isotherms were measured with a vapor sorption analyzer (VSA), a state-of-the-art instrument developed by METER Inc. [13]. A sample with a weight of 0.5–2 g was placed in the test cell, and the sample weight was measured at different relative humidity levels following wetting (adsorption) or drying (desorption). All performed test fulfil requirements for determination of sorption properties of building materials, set out in [31].

Air permeability (μm^2) was determined by an air permeameter. This method is used within the field of soil material characterization [32]. The sample was placed in a sample ring, which was mounted in the air permeameter. A pressure difference of 0.1 mBar was applied over the two sides of the sample, and the airflow through the sample was measured. The gas permeability k was then calculated by applying Darcy's law [33]. Afterwards, the modified Rayleigh number, Ra_m, was calculated for Rockwool by the formula $Ra_m = 3 \cdot 10^6 \cdot \frac{d \cdot k \cdot \Delta T}{\lambda}$, where d is the thickness of the insulation material, k is the air permeability, ΔT is the temperature difference across the material and λ is the thermal conductivity [34].

Thermal conductivity was measured with a Guarded Hot Plate Apparatus (EP500, Lambda-Meßtechnik GmbH), which is a state-of-the-art method for determination of thermal conductivity [35]. The materials were conditioned at 21°C and 40% relative humidity (laboratory conditions) before measurements. A temperature gradient of 10 K was maintained between the two plates holding the material while the heat flux through the sample was measured. The thermal conductivity was determined for an average sample temperature of 20°C (upper plate temperature of 25°C and lower plate temperature of 15°C).

Table 1. Fibre materials and their characteristics.

Fibre material	Rockwool	Kevlar	PET fibres
	[table_11]	[table_12]	[table_13]
Producer	Rockwool™	DuPont™	Current study
Raw material	Basalt rock	Polyaramide	Polyethene terephthalate
Raw material density	2800–3000 kg/m^3 [21]	1440 kg/m^3 [22]	1380 kg/m^3 [23]
Production method	Melt blowing	Melt blowing	Electrospinning
Applications	Housing insulation [24], growth media [25], acoustic dampening [26], fire retarded floor separations [27]	Body armour fabric [28], ballistic composites [28], bicycle tires [29]	Polyester fibres in clothing, nonwoven mats [30]

Commercial names: Rockwool Flexibat 100® and Kevlar 49®.

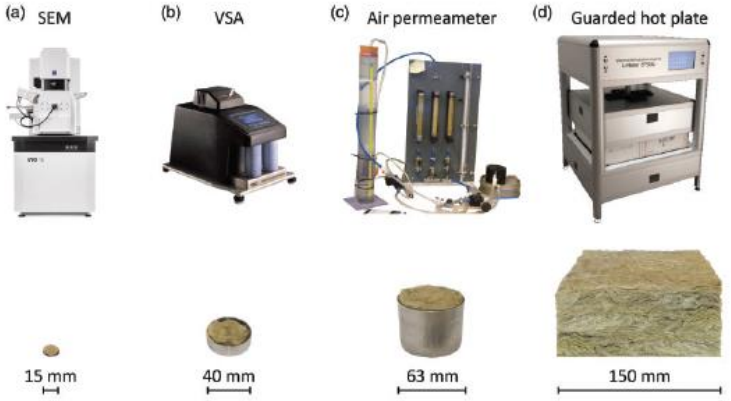

Figure 2. Instruments used for characterization of the material properties with a typical size of test samples for fibre materials. For illustration purposes, Rockwool® is used.

The typical measurement time of each method including sample preparation is: SEM – 30 min, VSA – 1–3 days, air permeameter – <10 min, guarded hotplate – 12 h.

Results and discussion

The microstructure characterization of the three fibre materials is presented in Figure 3. The length and diameter of the three types of fibre differ significantly.

The sorption-desorption isotherms of the three materials are presented in Figure 4. The Kevlar fibres exhibited the largest moisture adsorption and storage capabilities per mass, due to the hydrophilic polyaramide bulk material. There was also significant hysteresis (larger moisture content for the drying curve than the wetting curve) for the Kevlar fibres relative to the PET and Rockwool fibres. Furthermore, it was observed that the Rockwool and PET fibres are not water-active at 20–80% relative humidity, meaning that this fibre type will have similar properties under most moisture conditions. It can also be seen that this is not the case for Kevlar, which could be a topic for further studies. These results suggest that for Rockwool and PET fibres relative humidity will most likely not have a significant influence on moisture adsorption. For Kevlar fibre materials, relative humidity may however have a large influence. In order to investigate the magnitude of the effect of moisture content further, more studies are required.

The results of the thermal conductivity of this study, together with the results of other studies [9,36,37] are shown in Figure 5. The Vieseh model of thermal conductivity as a function of density is given by $\lambda = 24.9118 + 0.0721 \cdot \rho^{0.91} + \frac{268.8436}{\rho}$.

	Rockwool	Kevlar	PET fibres
SEM overview	[figure3_11] 	[figure3_21] 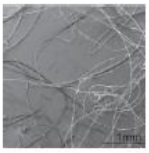	[figure3_31] 
SEM detailed close-up view	[figure3_12] 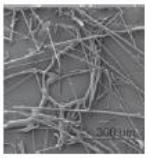	[figure3_22] 	[figure3_32] 
Typical range of fiber length	$[1-5]\cdot10^{-3}$ m	$[1-1.5]\cdot10^{1}$ m	$[1-2]\cdot10^{-1}$ m
Measured fiber diameter	6 µm +/- 2 µm	12 µm +/- 3 µm	33 µm +/- 4 µm
Fibre structure	Short, stiff fibres with no alignment	Long, flexible aligned fibres	Long, flexible fibres with no alignment

Figure 3. Images and microstructural characteristics for Rockwool, Kevlar and PET fibres.

It is seen that the results of all tests indicate a minimum thermal conductivity at a total volume content of solids between 0.025 and 0.050.

The results of the thermal conductivity and air permeability measurements can be seen in Figure 6. The experiments regarding thermal conductivity and air permeability were carried out at a constant air relative humidity of 40%. Consequently, the effect of moisture content on insulation materials was not considered. One can see that both the curves of thermal conductivity and air permeability with respect to porosity present an inflection point in the region between 0.025 and 0.050 of the total volume content of solid. At low total volume of solids, the thermal conductivity drops with increasing total volume content of solids. In this change zone, the thermal conductivity starts to rise again, and the air permeability drops more slowly. This is due to increased fibre contact, and hence more

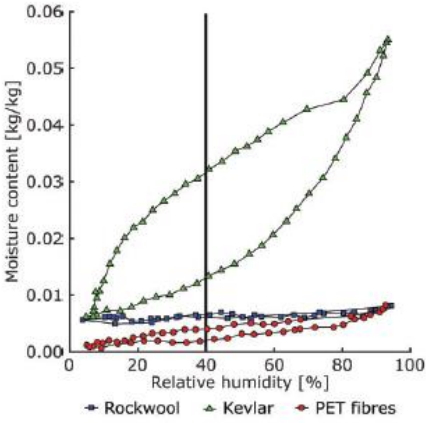

Figure 4. Water vapour adsorption and desorption isotherms for the three fibre materials. The vertical solid line at 40% relative humidity marks the laboratory ambient conditions while running of the thermal tests. Note the connected data points to show adsorption and desorption, and that these isotherms are similar for Rockwool.

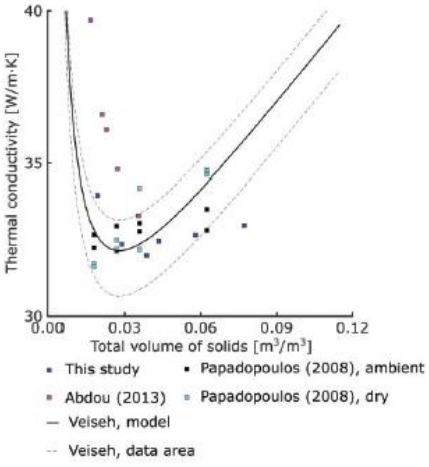

Figure 5. Thermal conductivity of Rockwool at different total volumes of solid from this study and other previous studies [9,36,37].

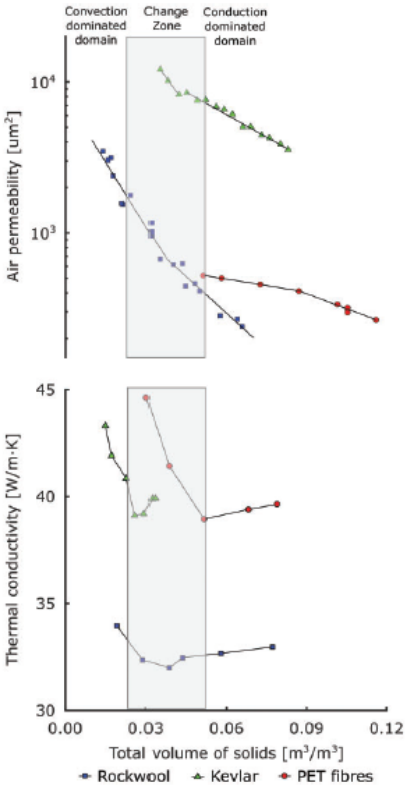

Figure 6. Thermal conductivity and air permeability as a function of volume content of solids for fibre materials. The shaded area is the change zone. The change point for PET fibres is marked at the first data point, as this measurement was in overflow. Note: Logarithmic y-axis for air permeability, and tendency lines for air permeability are piecewise exponential.

thermal bridges (increased thermal conductivity) and a more tortious pore network (lower gas permeability).

As the fibres become more compacted, the gas permeability decreases, and thermal conductivity becomes more dominant due to increased fibre contact. The convection of air becomes less dominant as the air permeability decreases,

and hence, the thermal transport shifts from convection-dominated to conduction-dominated as explained earlier.

As mentioned before, the moisture content in a material is a contributing factor to the connectivity between the fibres. As the fibres have a surface layer of water, liquid bridges develop between the fibres, leading to higher conduction than at a dry state. Furthermore, the water itself is more conductive than the air it has replaced. It should be noted that these experiments were performed at single relative humidity. Materials are expected to perform differently in a dry and humid atmosphere. The laboratory conditions of approximately 40% relative humidity are neither a dry nor a wet state, meaning that this one-point investigation is the middle ground. At drier states, the transition zone is expected to shift towards higher total volumes of solid, due to the lower number of liquid bridges and hence both lower conduction and more open pores network. The opposite is expected if the moisture content increases.

The Rayleigh number describes the relation between convective and conductive heat transfer in a porous media [38]. The modified Rayleigh number versus total volume content of solids for the Rockwool sample can be seen in Figure 7. The Rayleigh number was calculated at a temperature difference of 30°C and a thickness of 30cm. The number also changes in the same domain as described for the gas permeability and the thermal conductivity. If the modified Rayleigh number is above 2.5, further analysis and measurements of the convective heat flow are required, according to [34]. From the results, it is deduced that an increased

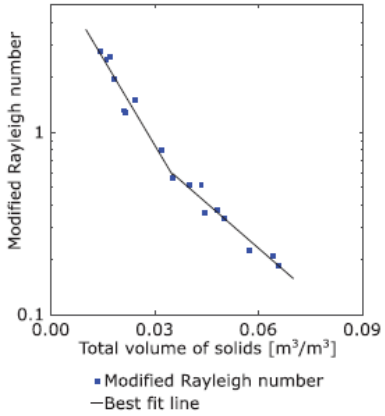

Figure 7. Modified Rayleigh number as a function of volume content of solids for Rockwool. Note: Logarithmic *y*-axis and tendency line is piecewise exponential.

total volume of solids can be used to improve the insulation performance and lower the modified Rayleigh number at the same time.

The novelty of this study is the combination of the different characterisation methods, all state of the art in their respective fields, and the combined overview of the transport properties in non-woven fibre materials. None of the references gives an overview of the correlation between heat, air and moisture characteristics for non-woven fibres, but woven fabrics have similar properties, as porosity and weaving pattern are closely interconnected [39]. This conclusion can be subject for further studies, where the mechanisms of the change in flow can be investigated.

The optimal density for thermal insulation is vastly explained for several materials, including fibre insulation materials and aerogels [36,40,41]. This shift, where conduction increases by increased fibre contact and decreased convection, is what this study describes as the change zone. Thermal conductivity and air permeability are linked together, as found for all three types of materials in this paper [5,39,42]. These studies concluded that thermal transfer and air permeability are connected, and proportional with static modified Rayleigh number.

The connection between thermal transfer and moisture content is well established for building materials [9,37,43] as well as for textiles [6,39]. The thermal conductivity increases with increased moisture content, as the conductive energy transfer increases. The link between permeability and moisture is also known in the clothing industry [44], where the increase of moisture content will decrease the gas permeability, as the fibres stick closer together. When this knowledge from the literature is combined with the results from this study, the change zone of a material can be described as a zone in a total volume content of solids, where transport through the fibres surpasses transport between the fibres.

As it is demonstrated that the gas permeability and the thermal conductivity experiences this shift in the change zone, this knowledge can be used for faster measurements and estimates of the thermal conductivity on basis of the gas permeability. The latter measurement can be performed in less than 10 min, including sample preparation, while the guarded hotplate measurement takes 12 h for a full characterisation. Furthermore, due to the nature of the measurement, gas permeability measurement might even be applied in real time, where e.g., a continuously produces lane of fibre material passes over an air outlet, and the flow on the other side of the lane is measured. This faster technique of quality control could be used to make more homogeneous quality, and hence reduce waste in the production facilities.

Conclusion

This study presents the concept of a transition zone which corresponds to the well-known optimal density for fibre material with regards to thermal insulation. This is also correlated with a change in gas permeability and modified Rayleigh number. This gained insight can be used for further development in thermal insulation

materials, as well as in rapid assessment of fibre insulation characteristics by mean of less time-consuming gas permeability test.

It is discussed that the moisture content of some fibre materials might change the value of this optimum density with minimum thermal conductivity. For the tested materials, the transition zone lies between 0.025 and 0.050 of total volume of solids. When the thermal conductivity increases at higher total volume contents of solids, the gas permeability starts to decrease less per unit volume content of solids.

Furthermore, Rockwool and PET fibres adsorbed small amounts of water between 20% and 80% relative humidity, while Kevlar adsorbed more. This corresponds to the fact that polyaramides, the Kevlar raw material, are hydrophilic, while PET and basalt are more hydrophobic. The results of this study will enable faster quality control through rapid gas permeability measurements, instead of the more time-consuming guarded hotplate measurements. With further research and engineering, this technique could be applicable for real-time measurements in an insulation manufacturing process.

Declaration of conflicting interests

The author(s) declared no potential conflicts of interest with respect to the research, authorship, and/or publication of this article.

Funding

The author(s) disclosed receipt of the following financial support for the research, authorship, and publication of this article: This work was supported by The Danish Board of Innovation (J. no. 0052-2012-3).

ORCID iD

Lasse Christiansen https://orcid.org/0000-0002-1771-3934

References

[1] Hagentoft C-E, Kalagasidis AS, Adl-Zarrabi B, et al. Assessment method of numerical prediction models for combined heat, air and moisture transfer in building components: benchmarks for one-dimensional cases. *J Therm Envel Build Sci* 2004; 27: 327–352.

[2] Jelle BP. Traditional, state-of-the-art and future thermal building insulation materials and solutions–properties, requirements and possibilities. *Energy Build* 2011; 43: 2549–2563.

[3] Frydrych I, Dziworska G and Bilska J. Comparative analysis of the thermal insulation properties of fabrics made of natural and man-made cellulose fibres. *Fibres Text East Eur* 2002; 10: 40–44.

[4] van der Tempel L. The effective temperature at which fingertips sense thermal effusivity and the bias of measurements at room temperature – ScienceDirect. *Measurement* 2019; 2019: 747–752.

[5] Barker RL, Guerth-Schacher C, Grimes R, et al. Effects of moisture on the thermal protective performance of firefighter protective clothing in low-level radiant heat exposures. *Text Res J* 2006; 76: 27–31.
[6] Zhiying C, Yanmin W and Weiyuan Z. Thermal protective performance and moisture transmission of firefighter protective clothing based on orthogonal design. *J Ind Text* 2010; 39: 347–356.
[7] Zach J, Korjenic A, Petránek V, et al. Performance evaluation and research of alternative thermal insulations based on sheep wool. *Energy Build* 2012; 49: 246–253.
[8] Latif E, Ciupala MA, Tucker S, et al. Hygrothermal performance of wood-hemp insulation in timber frame wall panels with and without a vapour barrier. *Build Environ* 2015; 92: 122–134.
[9] Karamanos A, Hadiarakou S and Papadopoulos A. The impact of temperature and moisture on the thermal performance of stone wool. *Energy Build* 2008; 40: 1402–1411.
[10] Arambakam R, Tafreshi HV and Pourdeyhimi B. Modeling performance of multicomponent fibrous insulations against conductive and radiative heat transfer. *Int J Heat Mass Transf* 2014; 71: 341–348.
[11] Churchill SW. Heat transfer by radiation through porous insulations. *AIChE J* 1959; 5: 8.
[12] Arthur E, Tuller M, Moldrup P, et al. Evaluation of a fully automated analyzer for rapid measurement of water vapor sorption isotherms for applications in soil science. *Soil Sci Soc Am J* 2014; 78: 754–760.
[13] Arthur E, Tuller M, Moldrup P, et al. Rapid and fully automated measurement of water vapor sorption isotherms: new opportunities for vadose zone research. *Vadose Zone J* 2014; 13: vzj2013.10.0185.
[14] Jones R, Pollock HM, Cleaver JA, et al. Adhesion forces between glass and silicon surfaces in air studied by AFM: effects of relative humidity, particle size, roughness, and surface treatment. *Langmuir* 2002; 18: 8045–8055.
[15] Quirk J and Murray R. Appraisal of the ethylene glycol monoethyl ether method for measuring hydratable surface area of clays and soils. *Soil Sci Soc Am J* 1999; 63: 839–849.
[16] Coelho M and Harnby N. The effect of humidity on the form of water retention in a powder. *Powder Technol* 1978; 20: 197–200.
[17] Jiřičková M, Pavlík Z, Fiala L, et al. Thermal conductivity of mineral wool materials partially saturated by water. *Int J Thermophys* 2006; 27: 1214–1227.
[18] Nagy B, Simon TK and Nemes R. Effect of built-in mineral wool insulations durability on its thermal and mechanical performance. *J Therm Anal Calorim* 2020; 139: 169. DOI: 10.1007/s10973-019-08384-5.
[19] Simon TK, Mlinárik L and Vargha V. Effect of water vapor on the compressive strength of a mineral wool insulation board. *J Build Phys* 2015; 39: 285–294.
[20] Dalton PD, Grafahrend D, Klinkhammer K, et al. Electrospinning of polymer melts: phenomenological observations. *Polymer* 2007; 48: 6823–6833.
[21] Stolper E and Walker D. Melt density and the average composition of basalt. *Contr Mineral and Petrol* 1980; 74: 7–12.
[22] Dupont Kevlar Technical Guide. Richmond (VA): Dupont, 2017.
[23] Brandrup J, Immergut EH, Grulke EA, et al. *Polymer handbook*. New York: Wiley, 1999.
[24] Xu J, Sugawara R, Widyorini R, et al. Manufacture and properties of low-density binderless particleboard from kenaf core. *J Wood Sci* 2004; 50: 62–67.

[25] Tu JC, Papadopoulos AP, Hao X, et al. The relationship of Pythium root rot and rhizosphere microorganisms in a closed circulating and an open system in rockwool culture of tomato. In: *International symposium on growing media and hydroponics 481*. 1997, pp. 577–586. International Society for Horticultural Science.
[26] Hummel AR and Swadley DL. *Noise abating brake shoe*. Google Patents, 1992.
[27] Balinski HA. *Fire-rated common area separation wall structure having break-away clips*. Google Patents, 1976.
[28] Lim CT, Shim VPW and Ng YH. Finite-element modeling of the ballistic impact of fabric armor. *Int J Impact Eng* 2003; 28: 13–31.
[29] Solomon TS. Systems for tire cord-rubber adhesion. *Rubber Chem Technol* 1985; 58: 561–576.
[30] Doshi J and Reneker DH. Electrospinning process and applications of electrospun fibers. *J Electrost* 1995; 35: 151–160.
[31] ISO 12571:2013. ISO 12571:2013, www.iso.org/cms/render/live/en/sites/isoorg/contents/data/standard/06/13/61388.html (2013, accessed 8 July 2019).
[32] Dane JH and Topp GC. *Methods of soil analyses: part 4 physical methods*. 2002. SSSA Book Ser. 5.4. SSSA, Madison, WI. DOI: 10.2136/sssabookser5.4.frontmatter
[33] Liu M, Wu J, Gan Y, et al. Evaporation limited radial capillary penetration in porous media. *Langmuir* 2016; 32: 9899–9904.
[34] ISO 10456:2008. DS/EN ISO 10456:2008 : Standard Distribute, https://sd-ds-dk.zorac.aub.aau.dk/Viewer?ProjectNr = M204192 (2008, accessed 26 June 2019).
[35] ISO 8302:1991. Thermal insulation – determination of steady-state thermal resistance and related properties – guarded hot plate apparatus, https://www.iso.org/standard/15422.html
[36] Veiseh S, Khodabandeh N and Hakkaki-Fard A. Mathematical models for thermal conductivity density relationship in fibrous thermal insulations for practical applications. *Asian J Civ Eng Build Hous* 2009; 10: 201–214.
[37] Abdou A and Budaiwi I. The variation of thermal conductivity of fibrous insulation materials under different levels of moisture content. *Constr Build Mater* 2013; 43: 533–544.
[38] Squires TM and Quake SR. Microfluidics: fluid physics at the nanoliter scale. *Rev Mod Phys* 2005; 77: 977–1026.
[39] Bedek G, Salaün F, Martinkovska Z, et al. Evaluation of thermal and moisture management properties on knitted fabrics and comparison with a physiological model in warm conditions. *Appl Ergon* 2011; 42: 792–800.
[40] Wang M, He J, Yu J, et al. Lattice boltzmann modeling of the effective thermal conductivity for fibrous materials. *Int J Therm Sci* 2007; 2007: 848–855.
[41] Diascorn N, Calas S, Sallee H, et al. Polyurethane aerogels synthesis for thermal insulation–textural, thermal and mechanical properties. *J Supercrit Fluids* 2015; 106: 76–84.
[42] Wahlgren P. Measurements and simulations of natural and forced convection in loose-fill attic insulation. *J Therm Envel Build Sci* 2002; 26: 93–109.
[43] Veiseh S and Sefidgar M. Prediction of effective thermal conductivity of moistened insulation materials by neural network. *Asian J Civ Eng* 2012; 13: 323–334.
[44] Gibson PW and Charmchi M. Modeling convection/diffusion processes in porous textiles with inclusion of humidity-dependent air permeability. *Int Commun Heat Mass Transf* 1997; 24: 709–724.

3.4. PAPER 4: RESUME OF UNPUBLISHED PAPER "MELT ELECTROSPINNING OF PET AND PET-AEROGEL FIBRES: AN EXPERIMENTAL AND MODELLING STUDY"

The last article, with the title "Melt electrospinning of PET and PET-aerogel fibres: An experimental and modelling study", is in review for publication, and hence a resume is included in the present dissertation. A preprint can be provided from the author.

The production of aerogel-polymer composites have been demonstrated by several techniques, including electrospinning (59,198), but such techniques can compromise the properties of the aerogel by wetting it with solvent. Furthermore, new insights into the process can be used to improve the technique even further (200).

To address these needs, this study investigates the electrospinning of polymer-aerogel composite fibres by pneumatic assistance of melt electrospinning. In addition, simulations of the electrospinning process are included in the study. These simulations examine the possibilities of using finite element simulation for these types of processes. This study presents melt electrospinning of PET and cellulose acetate butyrate fibres along with PET-aerogel composite fibres. Furthermore, and based on the experimental results, the paper proposes a logistic function as a viscosity model for molten PET polymers.

The experiments demonstrate that aerogel-PET composite fibres can be electrospun by pneumatically assisted electrospinning. This pneumatic assistance leads to an increase in fibre size. Furthermore, the use of finite element methods for simulation of the process is demonstrated using the logistic viscosity function and a method of parametric ramping.

The results prove the concept of pneumatic electrospinning for melt electrospinning and can be used to refine the technique further. In combination with the temperature-dependent finite element knowledge, it offers new insights into the electrospinning of polymer-aerogel composite materials.

CHAPTER 4. CONCLUSION

This PhD thesis has generated deeper insights into the electrospinning of composite materials. Firstly, novel production methods for aerogel-polymer composite fibres and their limits have been tested and described. Secondly, an increased understanding of the mechanism of heat transfer in nonwoven fibre materials has been obtained. The production methods for aerogel-polymer composite fibres can be divided into two main techniques: the solvent-based and the melt-based composite electrospinning. Both the solvent- and the melt-based techniques could be performed with airflow conveying the aerogel into the fibres. For solution electrospinning, apart from coaxial spinning, it was also demonstrated that composite fibres could be obtained from polymer-aerogel solution mixtures. The heat transfer mechanisms of electrospun fibres and reference materials were also investigated. During the investigation, it became evident that there were limitations to the use of fibre materials for insulation purposes in an atmospheric environment. The results revealed that a change-point occurred where the thermal transport shifted from the conductive to the convective regime.

The added knowledge to the field of electrospinning has also been updated. As electrospinning is evolving rapidly, new electrospinning variants, like presented here, can aid future innovation and science. Furthermore, the concept of the change zone described in the paper “Heat and air transport in differently compacted fibre materials” (199) gives rise to new insights within the field of fibre insulation materials.

The described techniques within this thesis, can both be upscaled to produce aerogel-polymer composite fibres on a larger scale, as well as being further developed into new materials combining another type of micro-particles into a polymer matrix.

CHAPTER 5. LITERATURE

1. Boys CV. On the Production, Properties, and some suggested Uses of the Finest Threads. Proc Phys Soc. 1887;9(8):8–19.

2. Taylor G. Electrically driven jets. In: Proceedings of the Royal Society of London A: Mathematical, Physical and Engineering Sciences. The Royal Society; 1969. p. 453–75.

3. Wilm MS, Mann M. Electrospray and Taylor-Cone theory, Dole's beam of macromolecules at last? International Journal of Mass Spectrometry and Ion Processes. 1994;136(2–3):167–80.

4. Reitz JR, Milford FJ, Christy RW. Foundations of Electromagnetic Theory. 4th ed. Vol. 1993. Addison Wesley; 630 p.

5. Bruus H. Theoretical microfluidics. Vol. 18. Oxford university press Oxford; 2008.

6. Conover W. Chemistry, (by Stephen S. Zumdahl and Susan A. Zumdahl). ACS Publications; 2009.

7. Cooley JF. Improved methods of and apparatus for electrically separating the relatively volatile liquid component from the component of relatively fixed substances of composite fluids. 6385, 1900. p. 19.

8. Yu D, Wang M, Li X, Liu X, Zhu L, Annie Bligh SW. Multifluid electrospinning for the generation of complex nanostructures. Wiley Interdisciplinary Reviews: Nanomedicine and Nanobiotechnology. 2019;e1601.

9. Kangazian Kangazi M, Gharehaghaji AA, Montazer M. Glass nanofibrous yarn through electrospinning along with in situ synthesis of silver nanoparticles. J Sol-Gel Sci Technol. 2018 Dec 1;88(3):528–40.

10. Mendes AC, Stephansen K, Chronakis IS. Electrospinning of food proteins and polysaccharides. Food Hydrocolloids. 2017;68:53–68.

11. Nonato RC, Morales AR, Vieira AF, Nista SVG, Mei LHI, Bonse BC. Solution parameters in the manufacture of ceramic ZnO nanofibers made by electrospinning. Applied Physics A. 2016(122.3):244.

12. Gupta P, Elkins C, Long TE, Wilkes GL. Electrospinning of linear homopolymers of poly(methyl methacrylate): exploring relationships between fiber

formation, viscosity, molecular weight and concentration in a good solvent. Polymer. 2005 Jun 17;46(13):4799–810.

13. Zhang YZ, Venugopal J, Huang Z-M, Lim CT, Ramakrishna S. Crosslinking of the electrospun gelatin nanofibers. Polymer. 2006 Apr 5;47(8):2911–7.

14. Chiu Y-J, Chi M-H, Liu Y-H, Chen J-T. Fabrication, Morphology Control, and Electroless Metal Deposition of Electrospun ABS Fibers. Macromol Mater Eng. 2016 Aug;301(8):895–901.

15. Zulfi A, Hapidin DA, Munir MM, Iskandar F, Khairurrijal K. The synthesis of nanofiber membranes from acrylonitrile butadiene styrene (ABS) waste using electrospinning for use as air filtration media. RSC advances. 2019;9(53):30741–51.

16. Matulevicius J, Kliucininkas L, Prasauskas T, Buivydiene D, Martuzevicius D. The comparative study of aerosol filtration by electrospun polyamide, polyvinyl acetate, polyacrylonitrile and cellulose acetate nanofiber media. Journal of Aerosol Science. 2016;92:27–37.

17. Zoccola M, Montarsolo Alessio, Aluigi A, Varesano A, Vineis C, Tonin C. Electrospinning of polyamide 6/modified-keratin blends. e-Polymers. 2007 Jan 1;7(1).

18. Chen H, Ma Q, Wang S, Liu H, Wang K. Morphology, compatibility, physical and thermo-regulated properties of the electrospinning polyamide 6 and polyethylene glycol blended nanofibers. Journal of Industrial Textiles. 2016;45(6):1490–503.

19. Feng Y, Xiong T, Xu H, Li C, Hou H. Polyamide-imide reinforced polytetrafluoroethylene nanofiber membranes with enhanced mechanical properties and thermal stabilities. Materials Letters. 2016;182:59–62.

20. Duan G, Liu S, Jiang S, Hou H. High-performance polyamide-imide films and electrospun aligned nanofibers from an amide-containing diamine. Journal of materials science. 2019;54(8):6719–27.

21. Cho D, Zhmayev E, Joo YL. Structural studies of electrospun nylon 6 fibers from solution and melt. Polymer. 2011;52(20):4600–9.

22. Carol P, Ramakrishnan P, John B, Cheruvally G. Preparation and characterization of electrospun poly(acrylonitrile) fibrous membrane based gel polymer electrolytes for lithium-ion batteries. Journal of Power Sources. 2011 Dec 1;196(23):10156–62.

23. Demir MM, Gulgun MA, Menceloglu YZ, Erman B, Abramchuk SS, Makhaeva EE, et al. Palladium Nanoparticles by Electrospinning from Poly(acrylonitrile- *co* -acrylic acid)−$PdCl_2$ Solutions. Relations between Preparation Conditions, Particle Size, and Catalytic Activity. Macromolecules. 2004 Mar;37(5):1787–92.

24. Ye P, Xu Z-K, Wu J, Innocent C, Seta P. Nanofibrous Membranes Containing Reactive Groups: Electrospinning from Poly(acrylonitrile- *c o* -maleic acid) for Lipase Immobilization. Macromolecules. 2006 Feb;39(3):1041–5.

25. Chen J-P, Ho K-H, Chiang Y-P, Wu K-W. Fabrication of electrospun poly(methyl methacrylate) nanofibrous membranes by statistical approach for application in enzyme immobilization. Journal of Membrane Science. 2009 Sep 15;340(1):9–15.

26. Macossay J, Marruffo A, Rincon R, Eubanks T, Kuang A. Effect of needle diameter on nanofiber diameter and thermal properties of electrospun poly(methyl methacrylate). Polym Adv Technol. 2007 Mar;18(3):180–3.

27. Chang H-Y, Chang C-C, Cheng L-P. Preparation of hydrophobic nanofibers by electrospinning of PMMA dissolved in 2-propanol and water. MATEC Web Conf. 2019;264:03004.

28. Brown TD, Dalton PD, Hutmacher DW. Melt electrospinning today: An opportune time for an emerging polymer process. Progress in Polymer Science. 2016 May 1;56:116–66.

29. Konwarh R, Karak N, Misra M. Electrospun cellulose acetate nanofibers: The present status and gamut of biotechnological applications. Biotechnology Advances. 2013 Jul 1;31(4):421–37.

30. Ma Z, Kotaki M, Ramakrishna S. Electrospun cellulose nanofiber as affinity membrane. Journal of Membrane Science. 2005 Nov 15;265(1):115–23.

31. Son WK, Youk JH, Lee TS, Park WH. Electrospinning of ultrafine cellulose acetate fibers: Studies of a new solvent system and deacetylation of ultrafine cellulose acetate fibers. Journal of Polymer Science Part B: Polymer Physics. 2004;42(1):5–11.

32. Son WK, Youk JH, Park WH. Antimicrobial cellulose acetate nanofibers containing silver nanoparticles. Carbohydrate Polymers. 2006 Sep 13;65(4):430–4.

33. Huang C, Niu H, Wu C, Ke Q, Mo X, Lin T. Disc-electrospun cellulose acetate butyrate nanofibers show enhanced cellular growth performances. J Biomed Mater Res. 2013 Jan;101A(1):115–22.

34. Ma J, Zhang Q, Mayo A, Ni Z, Yi H, Chen Y, et al. Thermal Conductivity of Electrospun Polyethylene Nanofibers. Nanoscale. 2015(40):16899–908.

35. Kohsari I, Shariatinia Z, Pourmortazavi SM. Antibacterial electrospun chitosan–polyethylene oxide nanocomposite mats containing bioactive silver nanoparticles. Carbohydrate polymers. 2016;140:287–98.

36. Lu C, Chiang SW, Du H, Li J, Gan L, Zhang X, et al. Thermal conductivity of electrospinning chain-aligned polyethylene oxide (PEO). Polymer. 2017 Apr 21;115:52–9.

37. Bolbasov EN, Buznik VM, Stankevich KS, Goreninskii SI, Ivanov YuN, Kondrasenko AA, et al. Composite Materials Obtained via Two-Nozzle Electrospinning from Polycarbonate and Vinylidene Fluoride/Tetrafluoroethylene Copolymer. Inorg Mater Appl Res. 2018 Mar;9(2):184–91.

38. Cho BM, Nam YS, Cheon JY, Park WH. Residual charge and filtration efficiency of polycarbonate fibrous membranes prepared by electrospinning. Journal of Applied Polymer Science. 2015;132(1).

39. Li Q, Xu Y, Wei H, Wang X. An electrospun polycarbonate nanofibrous membrane for high efficiency particulate matter filtration. RSC Advances. 2016;6(69):65275–81.

40. Qiu X, Lee BL-P, Ning X, Murthy N, Dong N, Li S. End-point immobilization of heparin on plasma-treated surface of electrospun polycarbonate-urethane vascular graft. Acta biomaterialia. 2017;51:138–47.

41. Qing W, Shi X, Deng Y, Zhang W, Wang J, Tang CY. Robust superhydrophobic-superoleophilic polytetrafluoroethylene nanofibrous membrane for oil/water separation. Journal of Membrane Science. 2017 Oct 15;540:354–61.

42. Zhao P, Soin N, Prashanthi K, Chen J, Dong S, Zhou E, et al. Emulsion Electrospinning of Polytetrafluoroethylene (PTFE) Nanofibrous Membranes for High-Performance Triboelectric Nanogenerators. ACS Appl Mater Interfaces. 2018 Feb 14;10(6):5880–91.

43. Huang Y, Huang Q-L, Liu H, Zhang C-X, You Y-W, Li N-N, et al. Preparation, characterization, and applications of electrospun ultrafine fibrous PTFE porous membranes. Journal of Membrane Science. 2017 Feb 1;523:317–26.

44. Ballard RL, Anneaux BL, Puckett SD, Manasco JL, Garner DP. Electrospun ptfe encapsulated stent and method of manufacture. 14/967,597, 2016.

45. Číková E, Kuliček J, Janigová I, Omastová M. Electrospinning of ethylene vinyl acetate/Poly (Lactic Acid) blends on a water surface. Materials. 2018;11(9):1737.

46. Kenawy E-R, Layman JM, Watkins JR, Bowlin GL, Matthews JA, Simpson DG, et al. Electrospinning of poly(ethylene-co-vinyl alcohol) fibers. Biomaterials. 2003 Mar 1;24(6):907–13.

47. Kotsuchibashi Y, Ebara M. Facile functionalization of electrospun poly (ethylene-co-vinyl alcohol) nanofibers via the benzoxaborole-diol interaction. Polymers. 2016;8(2):41.

48. Lee H-J, Lim J-M, Kim H-W, Jeong S-H, Eom S-W, Hong YT, et al. Electrospun polyetherimide nanofiber mat-reinforced, permselective polyvinyl alcohol composite separator membranes: A membrane-driven step closer toward rechargeable zinc–air batteries. Journal of Membrane Science. 2016 Feb 1;499:526–37.

49. Bagheri H, Rezvani O, Banihashemi S. Core–shell electrospun polybutylene terephthalate/polypyrrole hollow nanofibers for micro-solid phase extraction. Journal of Chromatography A. 2016;1434:19–28.

50. Bagheri H, Najafi Mobara M, Roostaie A, Baktash MY. Electrospun magnetic polybutylene terephthalate nanofibers for thin film microextraction. Journal of separation science. 2017;40(19):3857–65.

51. Bagheri H, Khanipour P, Asgari S. Magnetic field assisted μ-solid phase extraction of anti-inflammatory and loop diuretic drugs by modified polybutylene terephthalate nanofibers. Analytica chimica acta. 2016;934:88–97.

52. Katsogiannis KAG, Vladisavljević GT, Georgiadou S. Porous electrospun polycaprolactone (PCL) fibres by phase separation. European Polymer Journal. 2015;69:284–95.

53. Suwantong O. Biomedical applications of electrospun polycaprolactone fiber mats. Polymers for Advanced Technologies. 2016;27(10):1264–73.

54. Wang Y, Zhang Y, Zhang Z, Su Y, Wang Z, Dong M, et al. An injectable high-conductive bimaterial scaffold for neural stimulation. Colloids and Surfaces B: Biointerfaces. 2020;195:111210.

55. Govinna ND, Keller T, Schick C, Cebe P. Melt-electrospinning of poly(ether ether ketone) fibers to avoid sulfonation. Polymer. 2019 May 8;171:50–7.

56. Wang L, Dou L, Guan G. Preparation of Sulfonated Poly(aryl ether sulfone) Electrospun Mat/Phosphosilicate Composite Proton Exchange Membrane. Journal of Electronic Materials; Warrendale. 2017 Mar;46(3):1883–8.

57. Cheng Y, Wang C, Zhong J, Lin S, Xiao Y, Zhong Q, et al. Electrospun polyetherimide electret nonwoven for bi-functional smart face mask. Nano Energy. 2017 Apr 1;34:562–9.

58. Mahar FK, Mehdi M, Qureshi UA, Brohi KM, Zahid B, Ahmed F, et al. Dyeability of recycled electrospun polyethylene terephthalate (PET) nanofibers: Kinetics and thermodynamic study. Journal of Molecular Liquids. 2017 Dec 1;248:911–9.

59. Christiansen L, Jensen LR, Fojan P. Electrospinning of nonwoven aerogel-polyethene terephthalate composite fiber mats by pneumatic transport. Journal of Composite Materials. 2019;53(17):2361–6.

60. Ding Y, Hou H, Zhao Y, Zhu Z, Fong H. Electrospun polyimide nanofibers and their applications. Progress in Polymer Science. 2016 Oct 1;61:67–103.

61. Shayapat J, Chung OH, Park JS. Electrospun polyimide-composite separator for lithium-ion batteries. Electrochimica Acta. 2015 Jul 10;170:110–21.

62. Selatile MK, Ray SS, Ojijo V, Sadiku R. Depth filtration of airborne agglomerates using electrospun bio-based polylactide membranes. Journal of Environmental Chemical Engineering. 2018 Feb 1;6(1):762–72.

63. Yang T, Wu D, Lu L, Zhou W, Ming Z. Electrospinning of polylactide and its composites with carbon nanotubes. Polymer Composites. 32(8):1280–8.

64. Fang X, Wyatt T, Shi J, Yao D. Fabrication of high-strength polyoxymethylene fibers by gel spinning. J Mater Sci. 2018 Aug 1;53(16):11901–16.

65. Hympánová L, Rynkevic R, Román S, Mori da Cunha MGMC, Mazza E, Zündel M, et al. Assessment of Electrospun and Ultra-lightweight Polypropylene Meshes in the Sheep Model for Vaginal Surgery. European Urology Focus. 2018 Jul 23;2020:190–8.

66. Shen Y, Liu Q, Deng B, Yao P, Xia S. Experimental study and prediction of the diameter of melt-electrospinning polypropylene fiber. Fibers Polym. 2016 Aug 1;17(8):1227–37.

67. Nogueira F, Teixeira P, Gouveia IC. Electrospinning polypropylene with an amino acid as a strategy to bind the antimicrobial peptide Cys-LC-LL-37. J Mater Sci. 2018 Mar 1;53(6):4655–64.

68. Ma X, Zhang L, Tan J, Qin Y, Chen H, He W, et al. Continuous manufacturing of nanofiber yarn with the assistance of suction wind and rotating collection via needleless melt electrospinning. Journal of Applied Polymer Science. 2017;134(20).

69. Ke H, Feldman E, Guzman P, Cole J, Wei Q, Chu B, et al. Electrospun polystyrene nanofibrous membranes for direct contact membrane distillation. Journal of Membrane Science. 2016 Oct 1;515:86–97.

70. Zhang Y-P, Yang J-H, Li L-L, Cui C-X, Li Y, Liu S-Q, et al. Facile Fabrication of Superhydrophobic Copper- Foam and Electrospinning Polystyrene Fiber for Combinational Oil–Water Separation. Polymers. 2019 Jan;11(1):97.

71. Zulfi A, Rezeki YA, Edikresnha D, Munir MM, Khairurrijal K. Synthesis of Fibers and Particles from Polyvinyl Chloride (PVC) Waste Using Electrospinning. IOP Conf Ser: Mater Sci Eng. 2018 May;367:012014.

72. Zhong Z, Cao Q, Jing B, Wang X, Li X, Deng H. Electrospun PVdF–PVC nanofibrous polymer electrolytes for polymer lithium-ion batteries. Materials Science and Engineering: B. 2012;177(1):86–91.

73. Kong L, Ziegler GR. Fabrication of pure starch fibers by electrospinning. Food Hydrocolloids. 2014;36:20–5.

74. Zhang X, Reagan MR, Kaplan DL. Electrospun silk biomaterial scaffolds for regenerative medicine. Advanced drug delivery reviews. 2009;61(12):988–1006.

75. Padrão J, Machado R, Casal M, Lanceros-Méndez S, Rodrigues LR, Dourado F, et al. Antibacterial performance of bovine lactoferrin-fish gelatine electrospun membranes. International journal of biological macromolecules. 2015;81:608–14.

76. Reddy CS, Arinstein A, Avrahami R, Zussman E. Fabrication of thermoset polymer nanofibers by co-electrospinning of uniform core-shell structures. J Mater Chem. 2009 Oct 1;19(39):7198–201.

77. Kawahara Y. Electrospinning of Direct Carbonizable Phenolic Resin-based Nanofibers. J Textile Sci Eng. 2016;6(3):257.

78. Haerst M, Seitz V, Ahrens M, Boudot C, Wintermantel E. Silicone Fiber Electrospinning for Medical Applications. 6th European Conference of the International Federation for Medical and Biological Engineering. 2015(45):537–40.

79. Wang H, Liu Z, Wang E, Zhang X, Yuan R, Wu S, et al. Facile preparation of superamphiphobic epoxy resin/modified poly (vinylidene fluoride)/fluorinated ethylene propylene composite coating with corrosion/wear-resistance. Applied Surface Science. 2015;357:229–35.

80. Megahed A, Zoalfakar SH, Hassan AE, Ali AA. A novel polystyrene/epoxy ultra-fine hybrid fabric by electrospinning. Polymers for Advanced Technologies. 2018;29(1):517–27.

81. Kameoka J, Verbridge SS, Liu H, Czaplewski DA, Craighead HG. Fabrication of Suspended Silica Glass Nanofibers from Polymeric Materials Using a Scanned Electrospinning Source. Nano Lett. 2004 Nov 1;4(11):2105–8.

82. Praeger M, Saleh E, Vaughan A, Stewart WJ, Loh WH. Fabrication of nanoscale glass fibers by electrospinning. Appl Phys Lett. 2012 Feb 6;100(6):063114.

83. Kohoutek T, Pokorny M, Knotek P. Electrospinning of nanofibrous layers of As-S chalcogenide glass. Advanced Device Materials. 2017 Nov 24;3(1):1–6.

84. Mohtaram F, Borhani S, Ahmadpour M, Fojan P, Behjat A, Rubahn H-G, et al. Electrospun ZnO nanofiber interlayers for enhanced performance of organic photovoltaic devices. Solar Energy. 2020;197:311–6.

85. Zhao Y, Li X, Dong L, Yan B, Shan H, Li D, et al. Electrospun SnO2–ZnO nanofibers with improved electrochemical performance as anode materials for lithium-ion batteries. International Journal of Hydrogen Energy. 2015 Nov 2;40(41):14338–44.

86. Qin N, Xiong J, Liang R, Liu Y, Zhang S, Li Y, et al. Highly efficient photocatalytic H2 evolution over MoS2/CdS-TiO2 nanofibers prepared by an electrospinning mediated photodeposition method. Applied Catalysis B: Environmental. 2017 Mar 1;202:374–80.

87. Cadafalch Gazquez G, Smulders V, Veldhuis SA, Wieringa P, Moroni L, Boukamp BA, et al. Influence of Solution Properties and Process Parameters on the Formation and Morphology of YSZ and NiO Ceramic Nanofibers by Electrospinning. Nanomaterials. 2017 Jan;7(1):16.

88. Castkova K, Maca K, Sekaninova J, Nemcovsky J, Cihlar J. Electrospinning and thermal treatment of yttria doped zirconia fibres. Ceramics International. 2017 Jul 1;43(10):7581–7.

89. Wang B, Wang Y, Lei Y, Wu N, Gou Y, Han C. Tailoring of Porous Structure in Macro-Meso-Microporous SiC Ultrathin Fibers via Electrospinning Combined with Polymer-Derived Ceramics Route. Materials and Manufacturing Processes. 2016 Jul 26;31(10):1357–65.

90. Larsen G, Spretz R, Velarde-Ortiz R. Use of coaxial gas jackets to stabilize Taylor cones of volatile solutions and to induce particle-to-fiber transitions. Advanced Materials. 2004;16(2):166–9.

91. Li F, Zhao Y, Song Y. Core-shell nanofibers: nano channel and capsule by coaxial electrospinning. nanofibers. 2010;2:418–38.

92. Khalf A, Madihally SV. Recent advances in multiaxial electrospinning for drug delivery. European Journal of Pharmaceutics and Biopharmaceutics. 2017 Mar 1;112:1–17.

93. Duan G, Greiner A. Air-Blowing-Assisted Coaxial Electrospinning toward High Productivity of Core/Sheath and Hollow Fibers. Macromolecular Materials and Engineering. 2019;1800669.

94. Liu R, Cai N, Yang W, Chen W, Liu H. Sea-island polyurethane/polycarbonate composite nanofiber fabricated through electrospinning. Journal of Applied Polymer Science. 2010;116(3):1313–21.

95. Koenig K, Beukenberg K, Langensiepen F, Seide G. A new prototype melt-electrospinning device for the production of biobased thermoplastic sub-microfibers and nanofibers. Biomaterials research. 2019;23(1):10.

96. Kumar A, Wei M, Barry C, Chen J, Mead J. Controlling fiber repulsion in multijet electrospinning for higher throughput. Macromolecular Materials and Engineering. 2010;295(8):701–8.

97. Yang Y, Jia Z, Li Q, Hou L, Liu J, Wang L, et al. A shield ring enhanced equilateral hexagon distributed multi-needle electrospinning spinneret. IEEE Transactions on Dielectrics and Electrical Insulation. 2010;17(5).

98. Silva PES, Abreu FV de, Godinho MH. Shaping helical electrospun filaments: a review. Soft Matter. 2017 Oct 4;13(38):6678–88.

99. He X-X, Zheng J, Yu G-F, You M-H, Yu M, Ning X, et al. Near-Field Electrospinning: Progress and Applications. J Phys Chem C. 2017 Apr 27;121(16):8663–78.

100. Biagi G, Holmgaard T, Skovsen E. Near-field electrospinning of dielectric-loaded surface plasmon polariton waveguides. Optics express. 2013;21(4):4355–60.

101. Lim SH, Mao H-Q. Electrospun scaffolds for stem cell engineering. Advanced drug delivery reviews. 2009;61(12):1084–96.

102. Lu B, Wang Y, Liu Y, Duan H, Zhou J, Zhang Z, et al. Superhigh-throughput needleless electrospinning using a rotary cone as spinneret. small. 2010;6(15):1612–6.

103. Yarin A, Zussman E. Upward needleless electrospinning of multiple nanofibers. Polymer. 2004;45(9):2977–80.

104. Shaid A, Wang L, Padhye R, Jadhav A. Needleless Electrospinning and Electrospraying of Mixture of Polymer and Aerogel Particles on Textile. Advances in Materials Science and Engineering. 2018;2018.

105. Li Y, Dong A, He J. Innovation of Critical Bubble Electrospinning and Its Mechanism. Polymers. 2020;12(2):304.

106. El-Newehy MH, Al-Deyab SS, Kenawy E-R, Abdel-Megeed A. Nanospider Technology for the Production of Nylon-6 Nanofibers for Biomedical Applications. J Nanomaterials. 2011 Jan;2011:9:1-9:8.

107. Smit AE, Sanderson RD. Method and apparatus for the production of fine fibres [Internet]. US20140302245A1, 2014 [cited 2019 Aug 1]. Available from: https://patents.google.com/patent/US20140302245A1/en

108. Persano L, Camposeo A, Tekmen C, Pisignano D. Industrial upscaling of electrospinning and applications of polymer nanofibers: a review. Macromolecular Materials and Engineering. 2013;298(5):504–20.

109. Sarkar K, Gomez C, Zambrano S, Ramirez M, de Hoyos E, Vasquez H, et al. Electrospinning to Forcespinning™. Materials Today. 2010 Nov 1;13(11):12–4.

110. Haider A, Haider S, Kang I-K. A comprehensive review summarizing the effect of electrospinning parameters and potential applications of nanofibers in

biomedical and biotechnology. Arabian Journal of Chemistry. 2018 Dec 1;11(8):1165–88.

111. Ray SS, Chen S-S, Li C-W, Nguyen NC, Nguyen HT. A comprehensive review: electrospinning technique for fabrication and surface modification of membranes for water treatment application. RSC Adv. 2016 Sep 6;6(88):85495–514.

112. YFLOW. YFLOW® FIBEROLL ELECTROSPINNING MACHINE. 2019.

113. Cai M, He H, Zhang X, Yan X, Li J, Chen F, et al. Efficient Synthesis of PVDF/PI Side-by-Side Bicomponent Nanofiber Membrane with Enhanced Mechanical Strength and Good Thermal Stability. Nanomaterials. 2019 Jan;9(1):39.

114. Ren J, Blackwood KA, Doustgani A, Poh PP, Steck R, Stevens MM, et al. Melt-electrospun polycaprolactone strontium-substituted bioactive glass scaffolds for bone regeneration. Journal of Biomedical Materials Research Part A. 2014 Sep 1;102(9):3140–53.

115. Anand Ganesh V, Sreekumaran Nair A, Kumar Raut H, Michael Walsh T, Ramakrishna S. Photocatalytic superhydrophilic TiO 2 coating on glass by electrospinning. RSC Advances. 2012;2(5):2067–72.

116. Dalton PD, Grafahrend D, Klinkhammer K, Klee D, Möller M. Electrospinning of polymer melts: Phenomenological observations. Polymer. 2007;48(23):6823–33.

117. McCann, Jesse T., Marquez M, Xai Y. Melt Coaxial Electrospinning: A Versatile Method for the Encapsulation of Solid Materials and Fabrication of Phase Change Nanofibers. Nanoletters. 2006(6):2868–72.

118. Levit N, Tepper G. Supercritical CO2-assisted electrospinning. The Journal of Supercritical Fluids. 2004 Nov 1;31(3):329–33.

119. Wahyudiono, Machmudah S, Kanda H, Okubayashi S, Goto M. Formation of PVP hollow fibers by electrospinning in one-step process at sub and supercritical CO2. Chemical Engineering and Processing: Process Intensification. 2014 Mar 1;77:1–6.

120. Pirzada T, Arvidson SA, Saquing CD, Shah SS, Khan SA. Hybrid Silica–PVA Nanofibers via Sol–Gel Electrospinning. Langmuir. 2012 Apr 3;28(13):5834–44.

121. Kim YB, Cho D, Park WH. Electrospinning of poly (dimethyl siloxane) by sol–gel method. Journal of applied polymer science. 2009;114(6):3870–4.

122. Beckman EJ. Supercritical and near-critical CO2 in green chemical synthesis and processing. The Journal of Supercritical Fluids. 2004;28(2–3):121–91.

123. Khorshidi S, Solouk A, Mirzadeh H, Mazinani S, Lagaron JM, Sharifi S, et al. A review of key challenges of electrospun scaffolds for tissue-engineering applications. Journal of tissue engineering and regenerative medicine. 2016;10(9):715–38.

124. Varesano A, Carletto RA, Mazzuchetti G. Experimental investigations on the multi-jet electrospinning process. Journal of Materials Processing Technology. 2009;209(11):5178–85.

125. Cai X, Zhu P, Lu X, Liu Y, Lei T, Sun D. Electrospinning of very long and highly aligned fibers. Journal of Materials Science. 2017;52(24):14004–10.

126. Pan H, Li L, Hu L, Cui X. Continuous aligned polymer fibers produced by a modified electrospinning method. Polymer. 2006;47(14):4901–4.

127. Yao L, Haas TW, Guiseppi-Elie A, Bowlin GL, Simpson DG, Wnek GE. Electrospinning and stabilization of fully hydrolyzed poly (vinyl alcohol) fibers. Chemistry of Materials. 2003;15(9):1860–4.

128. Kameoka J, Craighead HG. Fabrication of oriented polymeric nanofibers on planar surfaces by electrospinning. Applied Physics Letters. 2003;83(2):371–3.

129. Feltz KP, Kalaf EAG, Chen C, Martin RS, Sell SA. A review of electrospinning manipulation techniques to direct fiber deposition and maximize pore size. Electrospinning. 2017;1(1):46–61.

130. Robinson TM, Hutmacher DW, Dalton PD. The next frontier in melt electrospinning: taming the jet. Advanced Functional Materials. 2019;29(44):1904664.

131. Rogers CM, Morris GE, Gould TW, Bail R, Toumpaniari S, Harrington H, et al. A novel technique for the production of electrospun scaffolds with tailored three-dimensional micro-patterns employing additive manufacturing. Biofabrication. 2014;6(3):035003.

132. Teo WE, Ramakrishna S. A review on electrospinning design and nanofibre assemblies. Nanotechnology. 2006;17(14):R89.

133. Afifi AM, Nakano S, Yamane H, Kimura Y. Electrospinning of continuous aligning yarns with a ‘funnel’target. Macromolecular Materials and Engineering. 2010;295(7):660–5.

134. Li D, Wang Y, Xia Y. Electrospinning Nanofibers as Uniaxially Aligned Arrays and Layer-by-Layer Stacked Films. Advanced Materials. 2004;16(4):361–6.

135. Chen L, Ameer A-S, Rea C, Mazeh H, Wu X, Chen W, et al. Preparation of electrospun nanofibers with desired microstructures using a programmed three-dimensional (3D) nanofiber collector. Materials Science and Engineering: C. 2020;106:110188.

136. Katta P, Alessandro M, Ramsier RD, Chase GG. Continuous Electrospinning of Aligned Polymer Nanofibers onto a Wire Drum Collector. Nano Lett. 2004 Nov 1;4(11):2215–8.

137. Szabó E, Démuth B, Nagy B, Molnár K, Farkas A, Szabó B, et al. Scaled-up preparation of drug-loaded electrospun polymer fibres and investigation of their continuous processing to tablet form. Express Polymer Letters. 2018 May;12(5):436–51.

138. Teo W-E, Gopal R, Ramaseshan R, Fujihara K, Ramakrishna S. A dynamic liquid support system for continuous electrospun yarn fabrication. Polymer. 2007 Jun 4;48(12):3400–5.

139. McCann JT, Marquez M, Xia Y. Highly Porous Fibers by Electrospinning into a Cryogenic Liquid. J Am Chem Soc. 2006 Feb 1;128(5):1436–7.

140. Li D, McCann JT, Xia Y. Use of Electrospinning to Directly Fabricate Hollow Nanofibers with Functionalized Inner and Outer Surfaces. Small. 2005 Jan 1;1(1):83–6.

141. Ahmadipourroudposht M, Fallahiarezoudar E, Yusof NM, Idris A. Application of response surface methodology in optimization of electrospinning process to fabricate (ferrofluid/polyvinyl alcohol) magnetic nanofibers. Materials Science and Engineering: C. 2015 May 1;50:234–41.

142. Jin Y, Yang D, Kang D, Jiang X. Fabrication of Necklace-like Structures via Electrospinning. Langmuir. 2010 Jan 19;26(2):1186–90.

143. Woignier T, Phalippou J, Hdach H, Larnac G, Pernot F, Scherer GW. Evolution of mechanical properties during the alcogel-aerogel-glass process. Journal of Non-Crystalline Solids. 1992;147:672–80.

144. Kanamori K, Aizawa M, Nakanishi K, Hanada T. New transparent methylsilsesquioxane aerogels and xerogels with improved mechanical properties. Advanced Materials. 2007;19(12):1589–93.

145. Arndt EM, Gawryla MD, Schiraldi DA. Elastic, low density epoxy/clay aerogel composites. Journal of Material Chemistry. 2007;17(33):3525–9.

146. Zhao S, Siqueira G, Drdova S, Norris D, Ubert C, Bonnin A, et al. Additive manufacturing of silica aerogels. Nature. 2020 Aug;584(7821):387–92.

147. Li L, Yalcin B, Nguyen BN, Meador MAB, Cakmak M. Flexible Nanofiber-Reinforced Aerogel (Xerogel) Synthesis, Manufacture, and Characterization. Applied materials and interfaces. 2009;2009(11):2491–501.

148. Deuber F, Mousavi S, Federer L, Hofer M, Adlhart C. Exploration of Ultralight Nanofiber Aerogels as Particle Filters: Capacity and Efficiency. ACS Appl Mater Interfaces. 2018 Mar 14;10(10):9069–76.

149. Si Y, Yu J, Tang X, Ge J, Ding B. Ultralight nanofibre-assembled cellular aerogels with superelasticity and multifunctionality. Nature Communications. 2014 Dec 16;5:5802.

150. Wu H, Chen Y, Chen Q, Ding Y, Zhou X, Gao H. Synthesis of flexible aerogel composites reinforced with electrospun nanofibers and microparticles for thermal insulation. Journal of Nanomaterials. 2013;2013:10.

151. Kittel Charles. Introduction to Solid State Physics. 8. edition. Hoboken, N.J: John Wiley & Sons; 2005.

152. Qu J, Cherkaoui M. Fundamentals of Micromechanics of Solids. Hoboken, NJ, USA: John Wiley & Sons, Inc; 2007.

153. Jones RM. Mechanics of composite materials /. 2nd ed. Philadelphia, PA: Taylor & Francis; 1999. 519 p.

154. Jelle BP. Traditional, state-of-the-art and future thermal building insulation materials and solutions–Properties, requirements and possibilities. Energy and Buildings. 2011;43(10):2549–63.

155. Official Journal of the European Union. Directive 2010/31/EU on the energy performance of buildings (recast) - 19 May 2010. Energy Performance of Buildings Directive Jun 18, 2010 p. 1–23.

156. Aditya L, Mahlia T, Rismanchi B, Ng H, Hasan M, Metselaar H, et al. A review on insulation materials for energy conservation in buildings. Renewable and Sustainable Energy Reviews. 2017;73:1352–65.

157. Lee SW, Lim CH, Salleh E@ IB. Reflective thermal insulation systems in building: A review on radiant barrier and reflective insulation. Renewable and Sustainable Energy Reviews. 2016 Nov 1;65:643–61.

158. Zhang Z, Wang K, Mo B, Li X, Cui X. Preparation and characterization of a reflective and heat insulative coating based on geopolymers. Energy and Buildings. 2015;87:220–5.

159. San Teh K, Yarbrough DW, Lim CH, Salleh E. Field evaluation of reflective insulation in south east Asia. Open Engineering. 2017;7(1):352–62.

160. Asan H. Investigation of wall's optimum insulation position from maximum time lag and minimum decrement factor point of view. Energy and Buildings. 2000 Jul 1;32(2):197–203.

161. Atkins Peter. Atkins' physical chemistry. 9. ed. Oxford: Oxford University Press; 2010.

162. Tritt TM. Thermal Conductivity: Theory, Properties, and Applications. Boston, MA: Springer US; 2004. (Springerlink, editor. Physics of Solids and Liquids).

163. Innocentini M, Salvini V, Pandolfelli V, Coury J. Permeability of ceramic foams. American Ceramic Society Bulletin. 1999;78(9):78–84.

164. Heinemann U. Influence of Water on the Total Heat Transfer in 'Evacuated' Insulations. International Journal of Thermophysics. 2008 Apr 1;29(2):735–49.

165. Haastrup S. Impact of Micro Silica on the Properties of Porous Calcium Silicate Products. 2018;

166. Sutcu M, Akkurt S. The use of recycled paper processing residues in making porous brick with reduced thermal conductivity. Ceramics International. 2009 Sep 1;35(7):2625–31.

167. Lopez Hurtado P, Rouilly A, Vandenbossche V, Raynaud C. A review on the properties of cellulose fibre insulation. Building and Environment. 2016 Feb 1;96:170–7.

168. Abdou A, Budaiwi I. The variation of thermal conductivity of fibrous insulation materials under different levels of moisture content. Construction and Building materials. 2013;43:533–44.

169. Veiseh S, Khodabandeh N, Hakkaki-Fard A. Mathematical models for thermal conductivity density relationship in fibrous thermal insulations for practical applications. Asian Journal of Civil Engineering (Building and Housing). 2009;10(2):201–14.

170. Veiseh S, Sefidgar M. Prediction of Effective Thermal Conductivity of Moistened Insulation Materials by Neural Network. Asian Journal of Civil Engineering. 2012;2012(13(3)).

171. Karamanos A, Hadiarakou S, Papadopoulos A. The impact of temperature and moisture on the thermal performance of stone wool. Energy and Buildings. 2008;40(8):1402–11.

172. Papadopoulos AM. State of the art in thermal insulation materials and aims for future developments. Energy and Buildings. 2005 Jan 1;37(1):77–86.

173. Hrubesh LW, Pekala RW. Thermal properties of organic and inorganic aerogels. Journal of Materials Research. 1994 Mar;9(3):731–8.

174. Wei G, Liu Y, Zhang X, Yu F, Du X. Thermal conductivities study on silica aerogel and its composite insulation materials. International Journal of Heat and Mass Transfer. 2011;54(11):2355–66.

175. Baetens R, Jelle BP, Gustavsen A. Aerogel insulation for building applications: A state-of-the-art review. Energy and Buildings. 2011 Apr 1;43(4):761–9.

176. Diascorn N, Calas S, Sallee H, Achard P, Rigacci A. Polyurethane aerogels synthesis for thermal insulation–textural, thermal and mechanical properties. The Journal of Supercritical Fluids. 2015;106:76–84.

177. Saeed S, Al-Sobaihi RM, Bertino MF, White LS, Saoud KM. Laser induced instantaneous gelation: aerogels for 3D printing. Journal of Materials Chemistry A. 2015;3(34):17606–11.

178. Liang Y, Wu H, Huang G, Yang J, Wang H. Thermal performance and service life of vacuum insulation panels with aerogel composite cores. Energy and Buildings. 2017 Nov 1;154:606–17.

179. Abdul Mujeebu M, Ashraf N, Alsuwayigh A. Energy performance and economic viability of nano aerogel glazing and nano vacuum insulation panel in multi-story office building. Energy. 2016 Oct 15;113:949–56.

180. Biener J, Stadermann M, Suss M, Worsley MA, Biener MM, Rose KA, et al. Advanced carbon aerogels for energy applications. Energy & Environmental Science. 2011;4(3):656–67.

181. An H, Wang Y, Wang X, Zheng L, Wang X, Yi L, et al. Polypyrrole/carbon aerogel composite materials for supercapacitor. Journal of Power Sources. 2010;195(19):6964–9.

182. Kabbour H, Baumann TF, Satcher JH, Saulnier A, Ahn CC. Toward new candidates for hydrogen storage: high-surface-area carbon aerogels. Chemistry of Materials. 2006;18(26):6085–7.

183. Iswar S, Griffa M, Kaufmann R, Beltran M, Huber L, Brunner S, et al. Effect of aging on thermal conductivity of fiber-reinforced aerogel composites: An X-ray tomography study. Microporous and Mesoporous Materials. 2019 Apr 1;278:289–96.

184. Insogel High Tech. Insogel Data Sheet. 2014.

185. Salimian S, Zadhoush A, Naeimirad M, Kotek R, Ramakrishna S. A review on aerogel: 3D nanoporous structured fillers in polymer-based nanocomposites. Polymer Composites. 2017;

186. Meador MAB, Malow EJ, Silva R, Wright S, Quade D, Vivod SL, et al. Mechanically strong, flexible polyimide aerogels cross-linked with aromatic triamine. ACS applied materials & interfaces. 2012;4(2):536–44.

187. Ryan AG, Kolzenburg S, Vona A, Heap MJ, Russell JK, Badger S. A proxy for magmatic foams: FOAMGLAS®, a closed-cell glass insulation. Journal of Non-Crystalline Solids: X. 2019;1:100001.

188. Li J, Zhuang X, Monfort E, Querol X, Llaudis AS, Font O, et al. Utilization of coal fly ash from a Chinese power plant for manufacturing highly insulating foam glass: Implications of physical, mechanical properties and environmental features. Construction and Building Materials. 2018;175:64–76.

189. König J, Petersen RR, Yue Y. Fabrication of highly insulating foam glass made from CRT panel glass. Ceramics international. 2015;41(8):9793–800.

190. Østergaard MB, Cai B, Petersen RR, König J, Lee PD, Yue Y. Effect of Macrostructure on Thermal Conductivity of Foam Glass. In 2018.

191. Ng S, Jelle BP, Sandberg LIC, Gao T, Wallevik ÓH. Experimental investigations of aerogel-incorporated ultra-high performance concrete. Construction and Building Materials. 2015 Feb 15;77:307–16.

192. Zheng T, Li A, Li Z, Hu W, Shao L, Lu L, et al. Mechanical reinforcement of a cellulose aerogel with nanocrystalline cellulose as reinforcer. RSC Advances. 2017;7(55):34461–5.

193. Nguyen S, Anthony DB, Qian H, Yue C, Singh A, Bismarck A, et al. Mechanical and physical performance of carbon aerogel reinforced carbon fibre hierarchical composites. Composites Science and Technology. 2019 Sep 29;182:107720.

194. Baetens R, Jelle BP, Thue JV, Tenpierik MJ, Grynning S, Uvsløkk S, et al. Vacuum insulation panels for building applications: A review and beyond. Energy and Buildings. 2010;42(2):147–72.

195. Kalnæs SE, Jelle BP. Phase change materials and products for building applications: A state-of-the-art review and future research opportunities. Energy and Buildings. 2015 May 1;94:150–76.

196. Bouquerel M, Duforestel T, Baillis D, Rusaouen G. Mass transfer modeling in gas barrier envelopes for vacuum insulation panels: A review. Energy and Buildings. 2012(55):903–20.

197. Bouquerel M, Duforestel T, Baillis D, Rusaouen G. Heat transfer modeling in vacuum insulation panels containing nanoporous silicas—A review. Energy and Buildings. 2012 Nov 1;54:320–36.

198. Christiansen L, Fojan P. Solution electrospinning of particle-polymer composite fibres. Manufacturing Review. 2016;3(21):1–6.

199. Christiansen L, Antonov YI, Jensen RL, Arthur E, de Jonge LW, Møldrup P, et al. Heat and air transport in differently compacted fibre materials. Journal of Industrial Textiles. 2020;1528083719900386.

200. Zhmayev E, Cho D, Joo YL. Modeling of melt electrospinning for semi-crystalline polymers. Polymer. 2010;51(1):274–90.

ISSN (online): 2446-1636
ISBN (online): 978-87-7210-908-4 AALBORG UNIVERSITY PRESS